

Contents lists available at [ScienceDirect](https://www.sciencedirect.com)

Review of Palaeobotany and Palynology

journal homepage: www.elsevier.com/locate/revpalbo

There and back again; on dinoflagellate cyst index events of the Eocene - Oligocene Transition in the (Para)Tethyan Realm[☆]

Henk Brinkhuis^{a,b,*}, Chiara Fioroni^c, Mustafa Yücel Kaya^d^a Department of Ocean Systems research (OCS), Royal Netherlands Institute for Sea Research (NIOZ), PO Box 1790, AB Den Burg, the Netherlands^b Department of Earth Sciences, Marine Palynology and Paleoceanography Group, Laboratory of Palaeobotany and Palynology, Faculty of Geosciences, Utrecht University, Princetonlaan 8a, 3584 CB Utrecht, the Netherlands^c Dipartimento di Scienze Chimiche e Geologiche, Università degli Studi di Modena e Reggio Emilia, Modena 41121, Italy^d Geological Institute, RWTH Aachen University, Aachen, Germany

ARTICLE INFO

Keywords:

Eocene–Oligocene transition
(Para)Tethys
Dinoflagellate cysts
Chronostratigraphy
Glacio-eustasy

ABSTRACT

A recent biochronostratigraphic (coccolithophorids, dinoflagellate cysts) and paleoenvironmental analysis of the hemipelagic deposits of the İhsaniye Formation, exposed along the cliffs in the Karaburun area (Black Sea coast, NW Turkey) provided new insights into the paleoceanographic and paleoclimatic evolution of the central (Para-) Tethyan region across the Eocene–Oligocene Transition (EOT). Among others, the study identified the Earliest Oligocene Stable Isotope Step (EOIS) marking the inception of Antarctica's first continental-scale ice sheets since the mid-Permian and coinciding with a major eustatic lowering, followed by the Early Oligocene Glacial Maximum (EOGM) period with its peak $\delta^{18}\text{O}$ values. The study showed apparent (quasi) continuity of the EOT succession at Karaburun, a notion that is not a 100% obvious from the organic walled dinoflagellate cyst (or dinocyst) record. This is mainly because the iconic Eocene – earliest Oligocene taxon *Areosphaeridium diktyoplokum*, in coeval sections in the region quite abundant near the end of the Eocene, is virtually absent. Here, we focus on obtaining a more detailed picture of correlative secondary dinocyst and other EOT bioevents allowing an even more robust chronostratigraphic assessment of the succession, including correlation to the Italian type sections. Particularly the ranges of the (herein taxonomically revised) species *Explostinium priabonensis* gen. and comb. nov. and the new species *Glaphyrocysta peterbijlii* sp. nov. may be regarded as additional criteria to correlate EOT strata within the (Para)Tethyan realm. Combined evidence now suggests that the Karaburun section may not be as complete as previously assumed and that a small part of the succession correlative to the base of the EOIS, representing a portion of the Adi dinocyst Zone may be missing. This aspect does not affect the overall outcome and significance of the studies at Karaburun. In fact, a brief hiatus may well be driven by the major EOT sea level lowering.

1. Introduction

Recently, the hemipelagic upper Eocene to lower Oligocene deposits of the İhsaniye Formation, exposed along the cliffs in the Karaburun area (Black Sea coast, NW Turkey) starred in an internationally coordinated integrated biochronostratigraphic and paleoenvironmental analysis, reported in [Kaya et al. \(2025\)](#). Notably the interbedded fine-grained deposits contain rich and diversified calcareous- and organic-walled microfossil associations, suitable for detailed biostratigraphic and biogeochemical (stable isotope) studies across the Eocene–Oligocene

boundary (EOB) ~33,8 Ma (cf. [Westerhold et al., 2020](#)). Indeed, the integrated study of the Karaburun section demonstrated the relative completeness of the sedimentary record and provided new insights into the paleoceanographic and paleoclimatic evolution of the central (Para-) Tethyan region across the Eocene–Oligocene Transition (EOT), including the identification of the Earliest Oligocene Stable Isotope Step (EOIS) and the Early Oligocene Glacial Maximum (EOGM) period with its peak $\delta^{18}\text{O}$ values (cf. [Hutchinson et al., 2021](#); [Kaya et al., 2025](#)). The EOIS marks the onset of the formation of the first stable continental ice sheets on the Antarctic continent since the mid Permian (e.g., [Zachos](#)

[☆] This article is part of a Special issue entitled: '60th Anniversary (invite only)' published in Review of Palaeobotany and Palynology.

* Corresponding author at: Department of Ocean Systems Research (OCS), Royal Netherlands Institute for Sea Research (NIOZ), PO Box 1790, AB Den Burg, the Netherlands.

E-mail address: henk.brinkhuis@nioz.nl (H. Brinkhuis).

<https://doi.org/10.1016/j.revpalbo.2025.105414>

Received 8 June 2025; Received in revised form 8 July 2025; Accepted 9 July 2025

Available online 16 July 2025

0034-6667/© 2025 The Authors. Published by Elsevier B.V. This is an open access article under the CC BY license (<http://creativecommons.org/licenses/by/4.0/>).

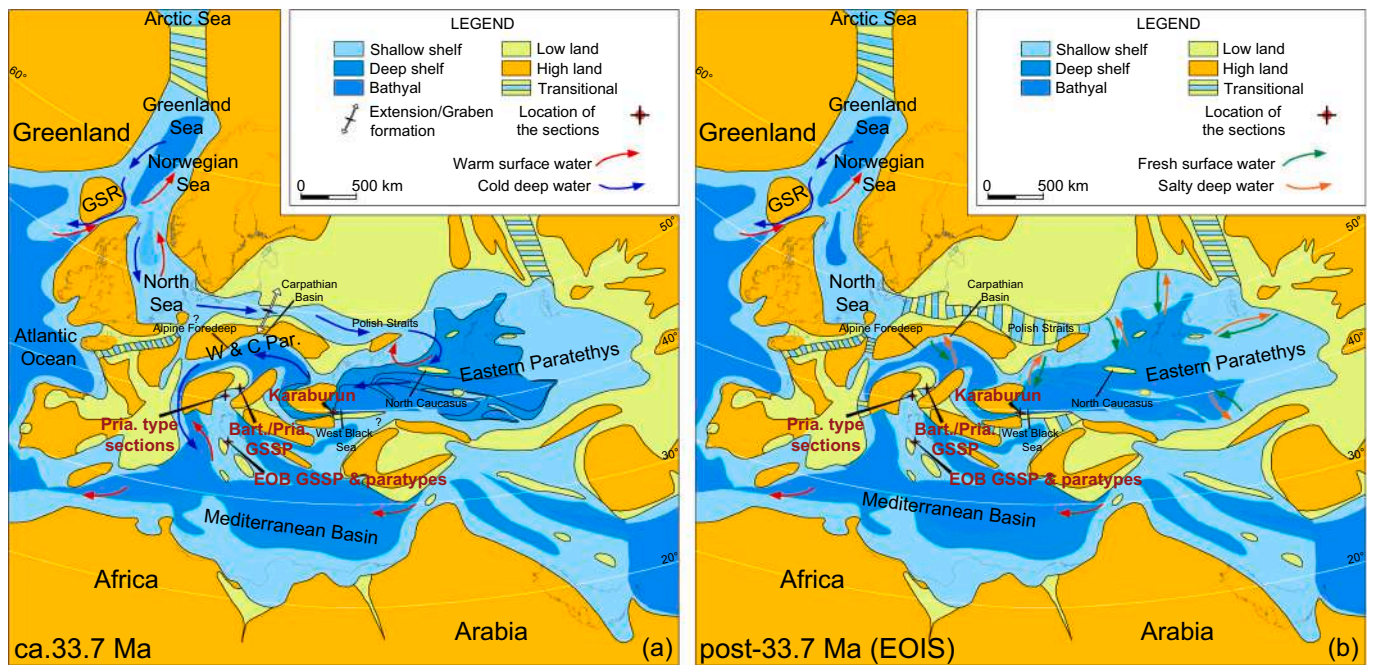


Fig. 1. Paleogeographic maps at 33.7 Ma and post-33.7 Ma (EOIS; modified from Kaya et al., 2025). (a) boreal water influx in a dominant anti-estuarine circulation the Paratethys, extending into the Mediterranean Tethys. GSR: Greenland Scotland Ridge. (b) dominant estuarine circulation in the Paratethys due to the geographic restrictions (consequences of the major sea-level lowering during the EOIS) and inferred hydrological changes (increased freshwater influx from land, all cf. Kaya et al., 2025). Approximate paleogeographic locations of (1) the NE Italian Priabonian Type sections (e.g., Brinkhuis, 1994), (2) the central Italian Massignano EOB GSSP and paratype sections (e.g., Hyland et al., 2009), and (3) the NE Italian Alano Bartonian/Priabonian GSSP (e.g., Agnini et al., 2021) are indicated as well.

et al., 2001; Westerhold et al., 2020), an important tipping point in Earth's climatic state, and major eustatic sea-level lowering. An important corollary of the study is the apparent (quasi-) continuity of the EOT succession at Karaburun, a notion that is not a 100% obvious from the dinocyst record.

Earlier studies into the organic walled dinoflagellate cyst (or 'dinocyst') distribution across the EOT in the central Mediterranean, and/or (Para-)Tethyan Realm (see Fig. 1a,b for approximate paleogeographic locations) indicate quite a dynamic state of the assemblages, with presumed mid to high latitude taxa making conspicuous first, or re-appearances in this climatically critical time interval in this lower latitude region (Brinkhuis and Biffi, 1993; Brinkhuis, 1994; van Mourik and Brinkhuis, 2005; Bati and Sancay, 2007; Houben et al., 2011; Bati, 2015; Sancay and Bati, 2020). In effect, the sole available otherwise well-calibrated EOT dinocyst zonation (as devised by Brinkhuis and Biffi, 1993) employs the subsequent (re) appearances of the mid latitude species *Achomosphaera alcicornu* (base Aal Zone) and *Glaphyrocysta semitecta* (base Gse Zone) in the region as index taxa for recognition of the Eocene/Oligocene (E/O) boundary interval. These events are calibrated against the succession of the Global Stratotype Section and Point (GSSP) of the E/O boundary at Massignano and other (paratype) sections in central Italy, as marked by the extinction of the hantkeninid-group of planktonic foraminifera, the principal criterion chosen by the International Commission of Stratigraphy (ICS; e.g., Premoli Silva et al., 1988; Hyland et al., 2009). Both mentioned dinocyst species are well known from various older Eocene deposits at higher northern latitude sites, including from the type Bartonian in the UK (e.g., Bujak, 1980). It was considered that their first occurrences in the Tethyan Realm reflect progressive climatic cooling by the end of the Eocene (e.g., Brinkhuis and Biffi, 1993; compare also Fig. 1a,b).

A next zonal boundary involves the Last Occurrence (LO) of the cosmopolitan, originally Southern Hemisphere, typical late Eocene species *Hemiplacophora semilunifera* (top Gse Zone), in turn followed by the LO of the well-known, long ranging, notably Northern Hemisphere early Eocene to earliest Oligocene species *Areosphaeridium diktyoplakum*

(top Adi Zone; cf. Brinkhuis and Biffi, 1993). While representatives of the former are quite frequent at Karaburun, only a few, small, possible fragments of the latter are found in the Turkish material (see Supplementary Information; SI, Table 1). This aspect hampers the confident recognition of the Adi Zone, with its body calibrated against the EOIS marking the onset of Antarctic glaciation in the central and NE Italian sections (Brinkhuis and Biffi, 1993; Brinkhuis, 1994; Brinkhuis and Visscher, 1995; van Mourik and Brinkhuis, 2005; Houben et al., 2011). Moreover, in all these Italian sections, this iconic EOT index species is a common member of the earliest Oligocene dinocyst assemblages, consistently present in sediments assigned to the Gse, and particularly, to the Adi Zone. Since the EOIS, and subsequent interval of heavy stable Oxygen isotope values (EOGM) is recognized at Karaburun (Kaya et al., 2025), and quite a large portion of it, the potential, at least partial, absence, and incompleteness of the Adi Zone is thus intriguing, and is possibly of consequence in further deliberations of the significance of the overall results of Kaya et al. (2025; see Fig. 2).

As it turns out, other dinocyst events characteristic for the EOT-interval, viz., occurring within the Aal, Gse, Adi, Rac to Cin zones of Brinkhuis and Biffi (1993), foremost comprise first and last occurrences of members of the Areoligeracean-family (formally: Areoligeraceae Evitt 1963) of typically 'dorso-ventrally compressed' cysts with an apical archaeopyle, type tA, and an 'offset sulcal notch' ('Gv-cysts' sensu Evitt, 1985). These include not only *Glaphyrocysta semitecta* itself, but also *Glaphyrocysta priabonensis*, '*Areoligera undulata*', '*Areoligera sentosa*' and *Licracysta?* (ex *Areoligera*) *semicirculata*-types (all sensu Brinkhuis and Biffi, 1993, and Brinkhuis, 1994, and cf. (Fensome et al., 2006), as they – besides in the central Italian sections – also occur in the type sections of the Priabonian Stage, NE Italy (Brinkhuis, 1994). In effect, these taxa are more abundant, and often even better preserved in the Karaburun sediments than ever seen in the Priabonian type material (see reports in Kaya et al., 2025, supplementary information, and HB, pers. obs.). In this fashion, the stratigraphic and (paleo)geographic distribution pattern of notably this group of taxa may shed light on the relative and absolute completeness of the Karaburun section, particularly of the EOT

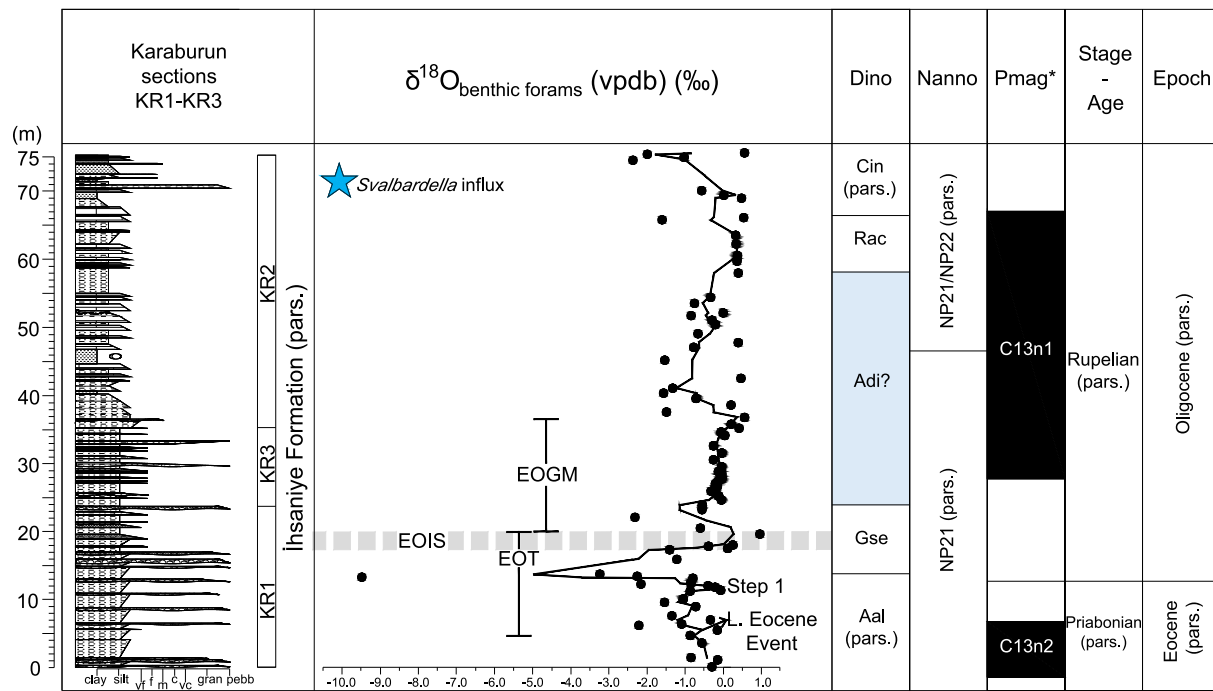


Fig. 2. Litho-, chemo- and chronostratigraphic overview and summary of the results of the integrated study of Kaya et al. (2025), based on correlations to the central Italian EOB GSSP at Massignano, and the paratype sections in the region (cf. Hyland et al., 2009). Pmag* = proposed correlation to the paleomagnetostratigraphy (chons) based on Brinkhuis and Biffi (1993) and Hyland et al. (2009) of the Karaburun dinocyst and calcareous nannoplankton studies from Kaya et al. (2025). Blue star indicates the position of the influx of the cold water dinocyst *Svalbardella cooksoniae* calibrated against basal Subchron C12r, close to the NP21/NP22 boundary. Marked in light blue is the questionable recognition of the Adi Zone, of particular importance to the Eocene – Oligocene Transition (EOT) interval, and central in the present study. EOGM: Early Oligocene Glacial Maximum, EOIS: Earliest Oligocene oxygen Isotope Step. (For interpretation of the references to color in this figure legend, the reader is referred to the web version of this article.)

interval currently questionably assigned to the Adi Zone (Fig. 2). Therefore, to further improve the Karaburun EOT age model and strengthen the correlation to the Italian type sections (including also the E/O GSSP section at Massignano) in particular, we focus here on the distribution patterns of these key EOT Areoligeracean dinoflagellate species.

2. Materials and methods

For details on location, lithology, sedimentology, palynological processing, and/or virtually any aspect of the sampled upper Eocene and lower Oligocene deposits in the Karaburun area we refer to the recent work of Kaya et al. (2025) and to Fig. 2. Following our initial studies (Kaya et al., 2025, see also their supplemental information, SI), for the purpose of the present study we focus on selected samples yielding the richest, and best preserved dinocyst assemblages, suitable for detailed morphological analysis (based on e.g., the ‘color-coding’ of the distribution chart presented in Kaya et al., 2025, SI). An updated marine palynological distribution chart for Karaburun is here included in the Supplemental Information, Table 1, and replaces the one earlier published in Kaya et al. (2025, SI).

Do note that, while organic-walled microfossil (or ‘palynomorph’) preservation and fragmentation varies significantly across the (sub) sections at Karaburun, the dominant palynological categories are (most often fragmented) organic linings of benthic foraminifera, organic walled dinoflagellate cysts (dinocysts), and sporomorphs (Kaya et al., 2025; see also SI). In addition, representatives of other aquatic algae like *Cyclopsiella*, *Pterospemella* and *Tasmanites* spp., occur throughout as well, as do small (<~20 µm) psilate- and skolochorate cysts (viz, ‘acritarchs’) of unknown affinity. Overall, the dinocyst assemblages are quite comparable to those known from neighboring regional EOT sections throughout the former Tethyan Realm (see, the overview provided in Kaya et al., 2025, and SI, Table 1).

In addition to the Karaburun material, we returned to the original palynological slides from the ‘Brinkhuis studies’ of central and NE Italy of the early 1990s for detailed comparison of the various Areoligeracean taxa in question, or we attempted to. To our disappointment, we found that anno 2025 only very few slides are still suited for light-microscopical analysis, including the type material of ‘*Glaphyrocysta priabonensis*’ of Brinkhuis (1994). Most have been oxidized and otherwise degraded in various ways. Also unfortunately, a quest to find the original ‘raw’ samples in the Utrecht GEO archives has not been successful so far, alas.

For dinocyst taxonomy, we refer to that cited in (Williams et al., 2019), except for Wetzelielloideae taxa (see discussion in Bijl et al., 2016). All materials are stored in the collection of the Marine Palaeoceanography and Palynology group (MPP), at the Laboratory of Palaeobotany and Palynology (Utrecht University, Faculty of Geosciences).

3. Results

Our renewed focus, and additional analyses of the above-mentioned set of EOT Areoligeracean taxa occurring in the Karaburun and Italian EOT sections led to several surprising new findings regarding the stratigraphic distribution, but also the morphology and related taxonomy of these species. Two prime examples involve (1) the notion that ‘*Glaphyrocysta priabonensis*’ as described by Brinkhuis (1994) from the Priabonian Type section – given the new Karaburun information – does actually *not* adhere to the generic definition of *Glaphyrocysta*, as it lacks an apical archaeopyle, nor, as it turns out, is it even an Areoligeracean, and must therefore be placed in another, new, genus described herein (‘*Explostinium*’ gen. nov.) characterized by a precingular archaeopyle, and (2) specimens assigned by Brinkhuis in 1994 to ‘*Areoligera undulata*’ and ‘*Areoligera sentosa*’ (both Eaton, 1976) and, more recently, to ‘*Glaphyrocysta* sp. A’ in Kaya et al. (2025; SI) in fact constitute a new species

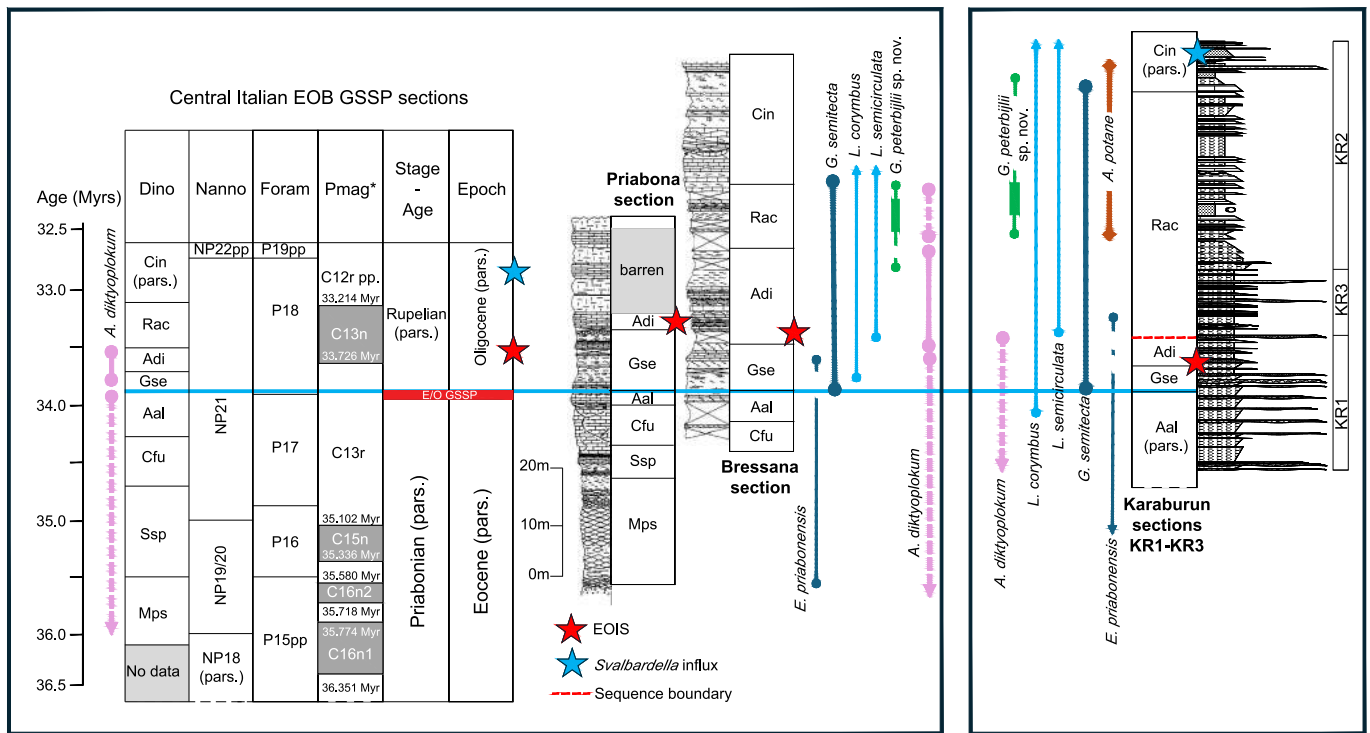


Fig. 3. Correlation panel combining the (old and new) key dinocyst data from the central and NE Italian sections with the findings of the Karaburun section of the same taxa. Red star indicates the EOIS. Blue star indicates the position of the influx of the cold water dinocyst *Svalbardella cooksoniae* calibrated against basal Subchron C12r, close to the NP21/NP22 boundary. The range of acritarch *Ascotomocystis potane* (known from the basal Rupelian type section in Belgium; Stover and Hardenbol, 1994) in samples from the sub-section KR2 at Karaburun is shown as well. (For interpretation of the references to color in this figure legend, the reader is referred to the web version of this article.)

of *Glaphyrocysta*, (*G. peterbiljii* sp. nov.). Both new entities are described below, in the taxonomic section. Other findings e.g., include the re-assignment of specimens listed as '*Licracysta* cf. *semicirculata*' in Kaya et al. (2025) and some of the specimens assigned to '*Glaphyrocysta*

intricata' and '*Areoligera semicirculata*' by Brinkhuis (1994) to *Licracysta corymbus* Fensome et al. (2006). Below, we discuss the distribution and consequences, per species, in a stratigraphic order, viz.:

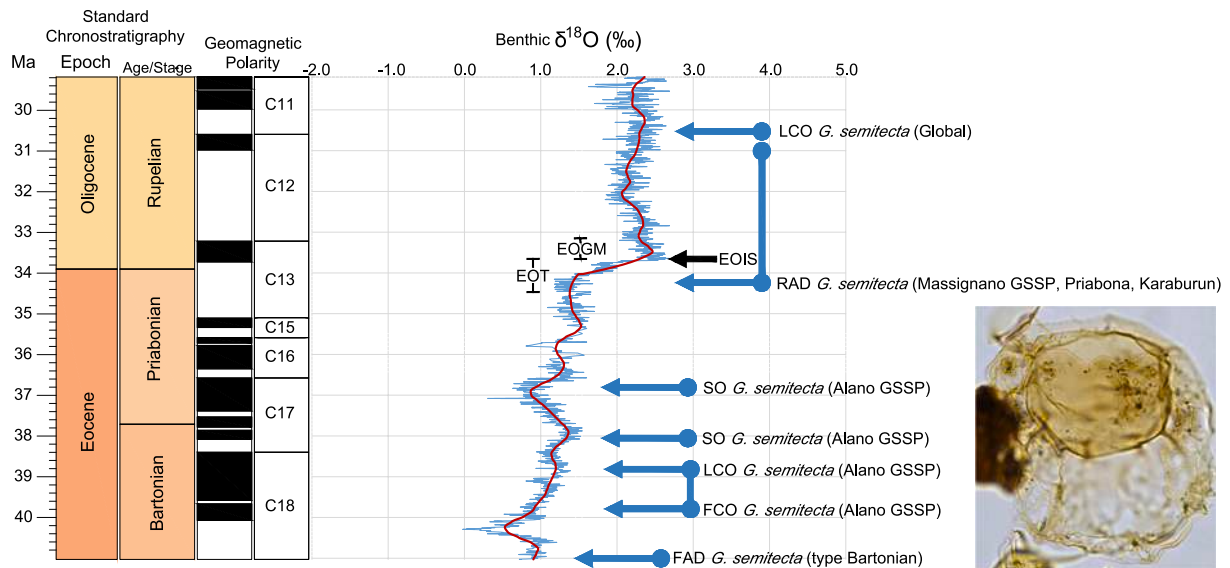


Fig. 4. Composite diagram of the late Eocene to early Oligocene part of the study of Westerhold et al. (2020), focusing on the chronostratigraphic alignment of their benthic $\delta^{18}\text{O}$ stable isotope data (mainly reflecting global intermediate to deeper water ocean temperatures and continental ice formation) and the distribution pattern of *Glaphyrocysta semitecta* in the (Para)Tethyan region (based on the data from Brinkhuis and Biffi, 1993; Brinkhuis, 1994; van Mourik and Brinkhuis, 2005; Bati and Sancay, 2007; Houben et al., 2011; Bati, 2015; Sancay and Bati, 2020, and Iakovleva, 2025). FAD = First Appearance Datum, FCO/LCO = First/Last Consistent Occurrence, SO = Spot Occurrence, RAD = Reappearance Datum. EOT: Eocene-Oligocene Transition, EOGM: Early Oligocene Glacial Maximum, EOIS: Earliest Oligocene oxygen Isotope Step. Calibration tie-points for the *G. semitecta* distribution vs magnetostratigraphy from Brinkhuis and Biffi (1993), Brinkhuis (1994), Sliwinska (2019), and Iakovleva (2025).

3.1. The total range of *Exploclinium* (Ex *Glaphyrocysta*) *priabonensis* gen. et comb. nov

While earlier designated as '*Glaphyrocysta* sp.' in Brinkhuis and Biffi (1993) from the central Italian material, this species was eventually described from the type section of the Priabonian Stage as *Glaphyrocysta priabonensis* in Brinkhuis (1994). In the otherwise well calibrated central Italian sections, it was found to occur throughout the Aal (consistent), and Gse zones (spot occurrences) of Brinkhuis and Biffi (1993). This mimics the pattern as found later in the Priabonian type sections (viz, at Priabona, and Bressana; cf. Brinkhuis, 1994; some of these could now be checked despite the disintegrating slides from the 1990s of some samples; see Fig. 3). More noteworthy, a similar, but not 100% the same distribution pattern is apparent in the Karaburun section, strengthening the assignment to the Aal and Gse zones of the interval between 0 and 18 m of section on the one hand, but with some spot occurrences until 35,25 m, now questionably assigned to the Adi Zone (Fig. 3) on the other (see also supplemental information). To our knowledge, this taxon has so far only been reported by other workers from a single sample at the top of the Gse Zone as recognized in the Kirmizitepe Section, Azerbaijan, South Caspian Basin (Bati, 2015, pl. IX, fig. 6). This is consistent with the other records but does not provide any further information regarding its stratigraphic range. Taken together, this species may for now be considered typical for the upper part of the classic Priabonian Stage, sporadically ranging into the very earliest Oligocene. The revised taxonomic aspects of the species are discussed further below, in the taxonomic section.

3.2. The total range of *Licracysta corymbus*

This species (see e.g., Figure Plate XVII) was first described from cuttings samples from wells drilled at the Grand Banks, Scotian Margin, offshore Newfoundland, Canada, and has a reported range top in the Rupelian, but an unknown base (Fensome et al., 2006). Re-examination of specimens from Priabona and Bressana from disintegrating slides (see Plate XX, figs. a, b) and earlier photographs (cf. Brinkhuis, 1994, pl. 1, figs. 1–2, as '*Glaphyrocysta intricata*', and pl. 1, figs. 4–7 as '*Areoligera semicirculata*'), and re-assessment of specimens listed as '*Licracysta* cf. *semicirculata*' in Kaya et al. (2025) led to designating them herein to *Licracysta corymbus*. The first appearance (i.e., near the Aal/Gse zonal boundary) is consistent between our records and add another correlative event for recognition of the E/O boundary sensu Premoli Silva et al. (1988). However, specimens with a somewhat similar morphology have been recovered from the late Bartonian to early Priabonian Alano section (as '*Licracysta?* sp'. Plate XXIV, figs. a, b; courtesy of Alina Iakovleva; see also Iakovleva, 2025). Hence, some issues regarding the actual First Appearance Datum (FAD) of the morphologies typical for *Licracysta* spp. remain.

3.3. The total range and distribution pattern of *Glaphyrocysta semitecta*

This species is first described from, and has a presumed FAD near the base of the type Bartonian in the UK (e.g., Bujak, 1980; Hooker and King, 2019; see Fig. 4). This while some reports indicate even slightly older occurrences in that area (at Whitecliff Bay, UK; A.I. Iakovleva, pers. obs., in Iakovleva, 2025). While subsequently widely reported from upper Eocene to lowermost Oligocene deposits of other high to mid latitude regions globally (see recent overview by Iakovleva, 2025), the consistent, but much younger First Occurrence (FO) of this cosmopolitan species in the Mediterranean Realm, was the basis for Brinkhuis and Biffi (1993) to employ it in their regional dinocyst zonation scheme (calibrated against Subchron C13r, just above the E/O GSSP boundary at Massignano, central Italy; Fig. 4). In turn, as the species is quite frequent in the EOT interval at Karaburun, its total range was recently used to recognize both the base of the Gse Zone as well as the top of the Rac Zone at that site (cf. Brinkhuis and Biffi, 1993; Kaya et al., 2025). This while

recently the study of the Alano Bartonian/Priabonian GSSP section (also NE Italy) however demonstrated that an older introduction of this species in the Mediterranean region occurred already much earlier, in late Bartonian times, in an interval calibrated against Subchron C18n2n (Iakovleva, 2025). As also noted by Iakovleva (2025), Brinkhuis and Biffi (1993) and Brinkhuis (1994) interpreted the apparent diachronous records of *G. semitecta* in the Mediterranean as reflecting long term Eocene climatic cooling, progressively 'pushing' the species towards lower (warmer) latitudes. The recent Alano data now suggest an even more complex pattern of incursions into lower (warmer) latitudes. Indeed, the spatial distribution now suggests not one, but multiple invasions (and temporary disappearances or 'retreats') of this taxon into lower latitude coastal seas and oceans apparently corresponding to stronger temperature variability (warmer and colder intervals) towards the end of the Eocene and overall climatic cooling (cf. Westerhold et al., 2020; see Fig. 4). Yet, the step we employ here, i.e. the one sensu Brinkhuis and Biffi (1993; defining the base of the Gse Zone) appears very robust indeed – as it aligns perfectly with the assignment of that critical interval at Karaburun to the EOIS (Kaya et al., 2025, see Fig. 4), as it also appears to do in sections further to the East (Bati and Sancay, 2007; Bati, 2015; Sancay and Bati, 2020). Moreover, also its final demise, defining the top of the Rac Zone sensu Brinkhuis and Biffi (1993), appears age-consistent across the Mediterranean and (Para) Tethys (e.g., Pross et al., 2010; Bati, 2015; Sancay and Bati, 2020; Kaya et al., 2025) and even higher latitude sections (e.g., in the North Sea Basin, van Simaeyns et al., 2005; Sliwinska, 2019).

One, perhaps significant, observation here is that the older specimens from Alano are, like the ones illustrated from the Bartonian Type (Bujak, 1980), characterized by a less smooth, more granulated when appressed, and more irregularly perforated when expanded, periphragm, relative to the younger ones from the EOT Gse, Adi and Rac zones in Italy and Turkey (e.g., compare the specimens illustrated on Plates XX–XXIII from Karaburun, Priabona and Alano). Further studies are needed to confirm the potential (eco)stratigraphic value of this notion. We conclude that for now, the consistent Mediterranean earliest Oligocene to mid early Oligocene (or Rupelian) range of this species is an important cornerstone for the chronostratigraphic assessment, and relative completeness of the Karaburun section.

3.4. The total range of *Licracysta?* *semicirculata*

This taxon (see e.g., Figure Plate XVIII and Plate XIX) originally *Areoligera*, later provisionally included in *Licracysta* by Fensome et al. (2006) can be regarded as a classic basal Oligocene (Rupelian) indicator, notably at mid northern latitude sites (e.g., van Simaeyns et al., 2005; Sliwinska, 2019). Also, its LO in the basal Chattian seems consistent throughout (e.g., Sliwinska, 2019) but falls outside the EOT interval of interest here. Its FAD is more elusive, since early occurrences are rare, and typically not ideally oriented specimens not straight-forward to identify. One issue with this species is its poor original description (Morgenroth, 1966) which does not really allow for confident identification, as earlier noted by (Fensome et al., 2006) as well. This may cause potential overlap between the two current species of *Licracysta* in the present materials and perhaps some confusion regarding their actual FADs in the late(st) Eocene and/or earliest Oligocene. Taken together, it appears that the FAD/FO of *Licracysta?* *semicirculata* is most consistent in the lower to middle part of the Adi Zone of Brinkhuis and Biffi (1993) between the Italian sections (Fig. 3). It follows, therefore that also its FO at Karaburun may hint to the presence of at least part of that zone there but appears to be delayed (Fig. 3).

3.5. The total range of *Glaphyrocysta peterbijlii* sp. nov.

Among the melee of these morphologically similar early Oligocene *Areoligeraceans*, our earlier analyses of the Karaburun samples identified yet another species of this group, noted in Kaya et al., 2025, as

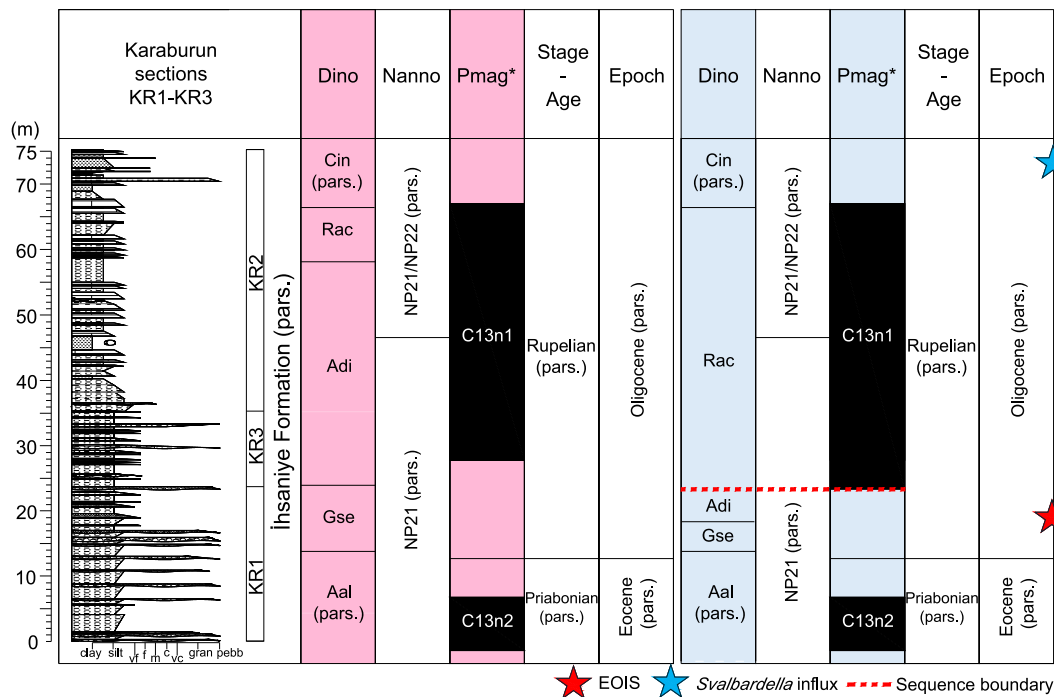


Fig. 5. Litho- and chronostratigraphic overview and summary of the results of the present study (blue) compared to the earlier work of Kaya et al. (2025; in pink). PMag* = proposed correlation to the paleomagnetostratigraphy (chrons) based on Brinkhuis and Biffi (1993) and Hyland et al. (2009) of the reassessed Karaburun dinocyst and calcareous nannoplankton studies from Kaya et al. (2025). Red star indicates the EOIS. Blue star indicates the position of the influx of the cold water dinocyst *Svalbardella cooksoniae* calibrated against basal Subchron C12r, close to the NP21/NP22 boundary. (For interpretation of the references to color in this figure legend, the reader is referred to the web version of this article.)

'*Glaphyrocysta* sp. A'. The reasonably to well-preserved dinocysts of the lower Oligocene interval at Karaburun now allow a robust characterization of this taxon and its morphological variability, that sets it apart from similar Areoligeraceans, below described as *Glaphyrocysta peterbijlii* sp. nov. Moreover, following best practices and possibilities using the degrading slides from the 1990s, it turns out that many (poorly preserved) specimens Brinkhuis (1994) at the time assigned to the overall morphologically very similar middle Eocene species *Areoligera undulata* and/or *Areoligera sentosa* of Eaton (1974), represent this (new) species (mainly from the Bressana section, see e.g., specimens shown of Plates XIV and XV). In addition, specimens depicted by Bati (2015, pl. X, figs. 10–11 as '? *Areoligera sentosa-tauloma*') from the Rupelian of Azerbaijan are herein considered conspecific with *G. peterbijlii*, rather than being elements 'reworked from the older Eocene' (cf. Bati, 2015).

Furthermore, based on the analysis of these kind of available illustrations resulting from dinoflagellate studies performed elsewhere (e.g., Köthe, 1990; van Simaey et al., 2005; Schiøler, 2005; Sliwinska, 2019) of the early Oligocene interval, this taxon appears to be so far exclusive for the Mediterranean – (Para-)Tethyan domain. Taken the reassessed information from NE Italy and Karaburun, NW Turkey, and Azerbaijan, the distribution pattern of *G. peterbijlii* is remarkably consistent between the sections, and typical for the Rac Zone, of mid Rupelian age (Fig. 3).

3.6. Completeness of the EOT interval of the Karaburun section, NW Turkey

The broad distribution patterns of the dinocyst species discussed above, and other relevant correlative elements across the EOT of the Italian and Turkish sections are shown in Fig. 3. An additional important chrono-biostratigraphic element is the total range of the acritarch *Ascotomocystis potane*. Although of unknown biological affinity, the finding of various specimens of this organic walled, likely aquatic algal taxon in samples from sub-section KR2 at Karaburun aids in assigning this interval to the basal Rupelian. The form is e.g., documented from

the basal Rupelian type section in Belgium (Stover and Hardenbol, 1994), but employed also further into the Paratethyan Realm, e.g., in eastern Anatolia to assign strata to the lower to mid Rupelian (Bati and Sancey, 2007; see also Fig. 3).

Regarding the stratigraphic distribution patterns of the additional dinocyst EOT 'index species', and associated events, when taken together (Fig. 3), it appears that the succession at Karaburun is as far as can be gauged, essentially complete. In fact, the quasi-absence of *Areosphaeridium diktyoplokum* in the lowermost Oligocene interval remains the sole argument for contemplating issues with the continuity of the succession. An additional line of evidence supporting this hypothesis is provided by the stratigraphic distribution of the identified nannofossil species (Fig. 2 and SI in Kaya et al., 2025). Although the lower Rupelian is generally characterized by a scarcity of nannofossil bioevents, no anomalous trends have been observed in the stratigraphic distribution of the recorded taxa. The Eocene–Oligocene boundary (EOB) is well identified by the onset of the acme of the *Clausiacoccus* group, (besides the FO of the dinocyst species *Glaphyrocysta semitecta*) which maintains consistent values up to the top of the studied interval, with several peaks that fall within the expected variability for the group, as documented at various sites (Viganò and Agnini, 2025). Similarly, no inconsistent patterns were observed in any of the other identified nannofossil species, supporting the conclusion that no significant discontinuities occur within the studied section. On this basis, it appears that only a very minor portion, or portions of the succession correlative to the Adi Zone may be missing at Karaburun. Conspicuously, the most likely candidate-horizon for a potential gap in the record coincides with the approximate position of a conglomerate layer at the base of the EOGM (i.e. at ca. 23,50 m in the KR section 1, just around the step to subsection KR3; Fig. 3), which could correspond to a sequence boundary related to the associated major eustatic sea level fall during the EOIS and EOGM (see also Kaya et al., 2025, for further supporting evidence). Increased sedimentation rates above this horizon, including the increased number of transported terrestrial and coastal elements (Kaya et al., 2025, and

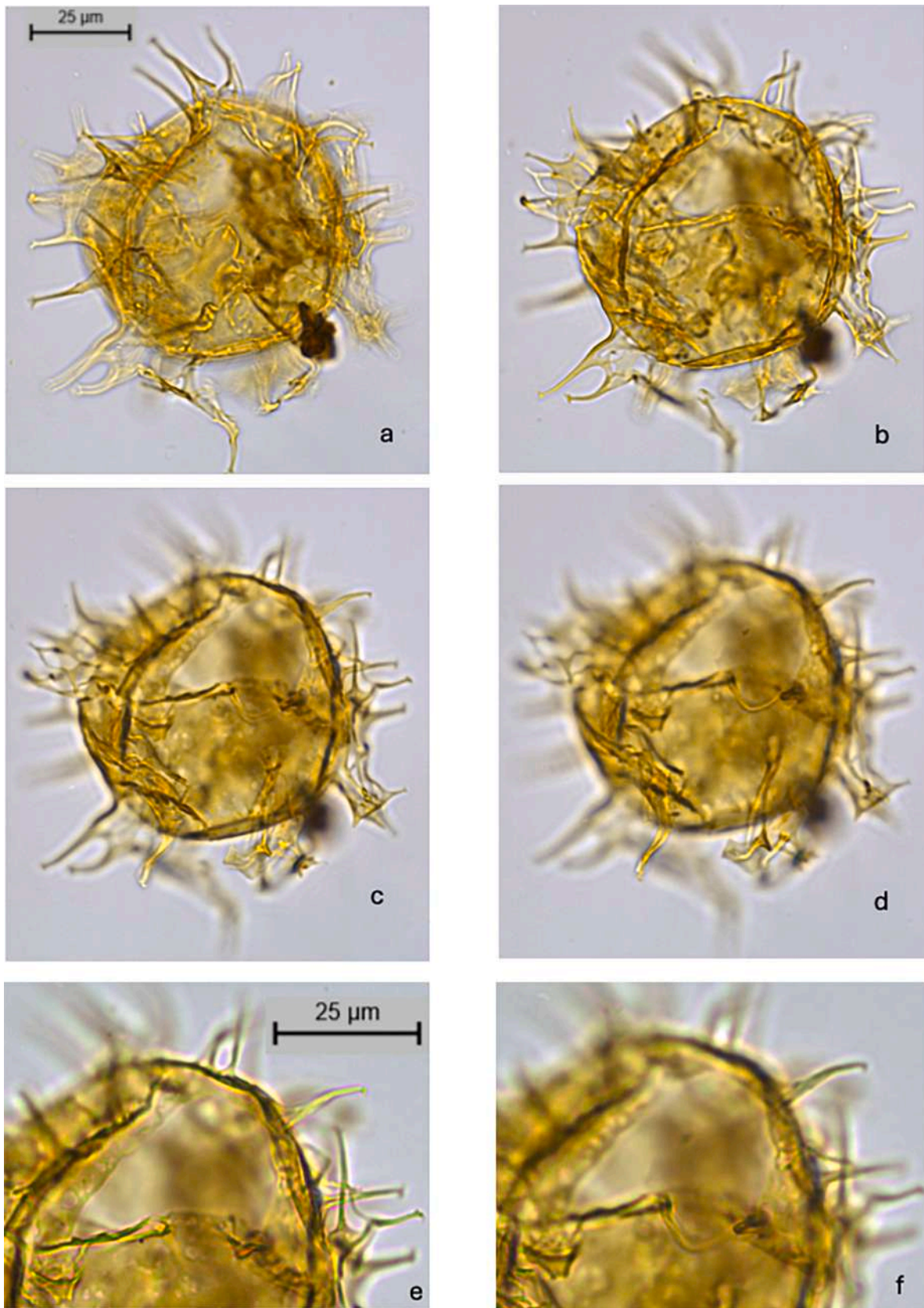


Plate I. a–d. *Explotinium priabonensis* gen. et comb. nov. high focus to low focus, from ventral to dorsal side. Neotype; sample KR22S1Y8, slide 2, EF: K42. e–f. idem. Detail of archaeopyle representing the loss of 3'; note the array of processes just adjacent to the archaeopyle margin, posteriorly.

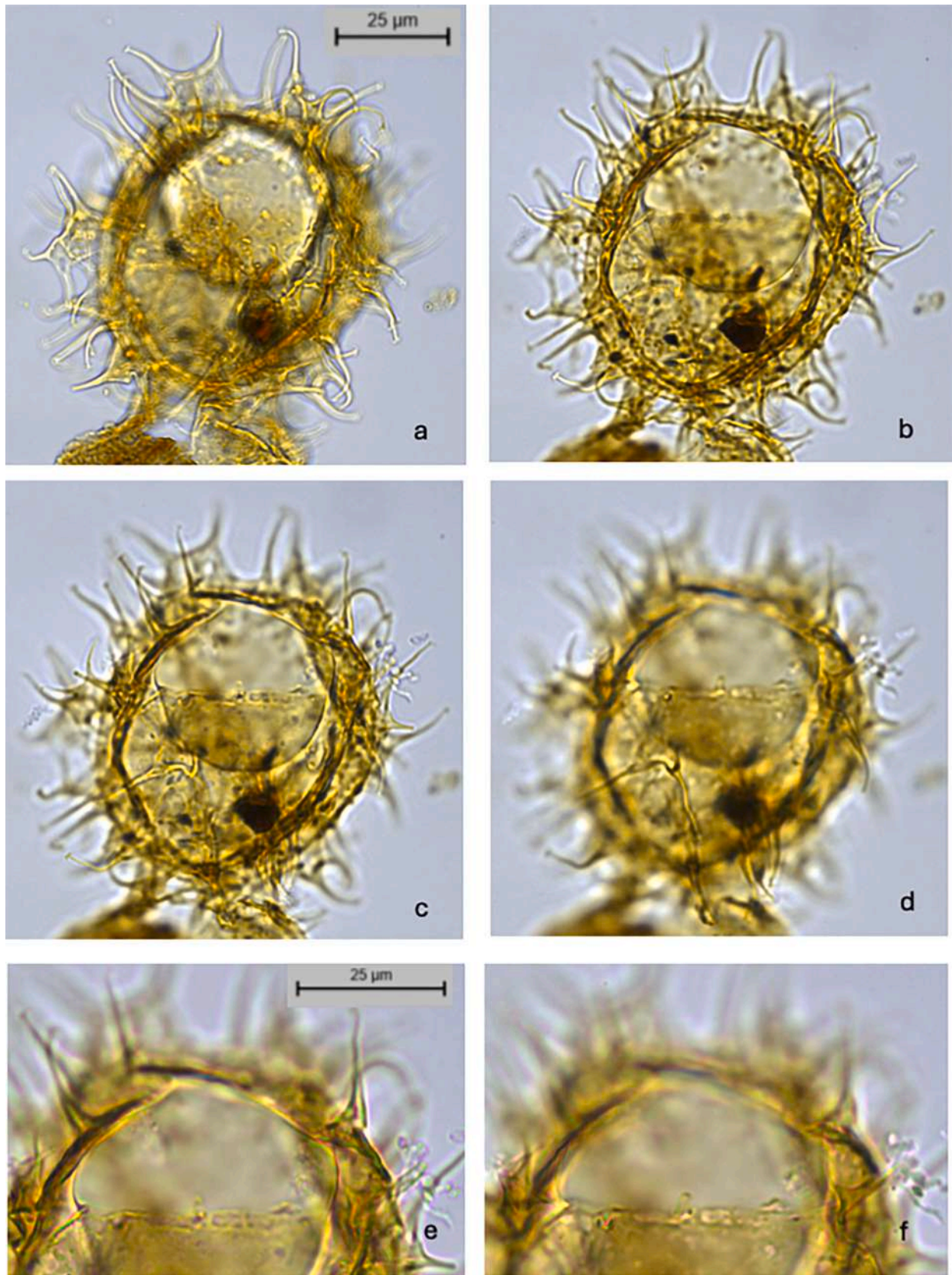


Plate II. a–d. *Explodinium priabonensis* gen. et comb. nov., high focus to low focus, from ventral to dorsal side. Paratype 1; sample KR22S1Y10, slide 1, EF: O9. e–f. idem. Detail of archaeopyle representing the loss of 3'; note the array of processes just adjacent to the archaeopyle margin, posteriorly.

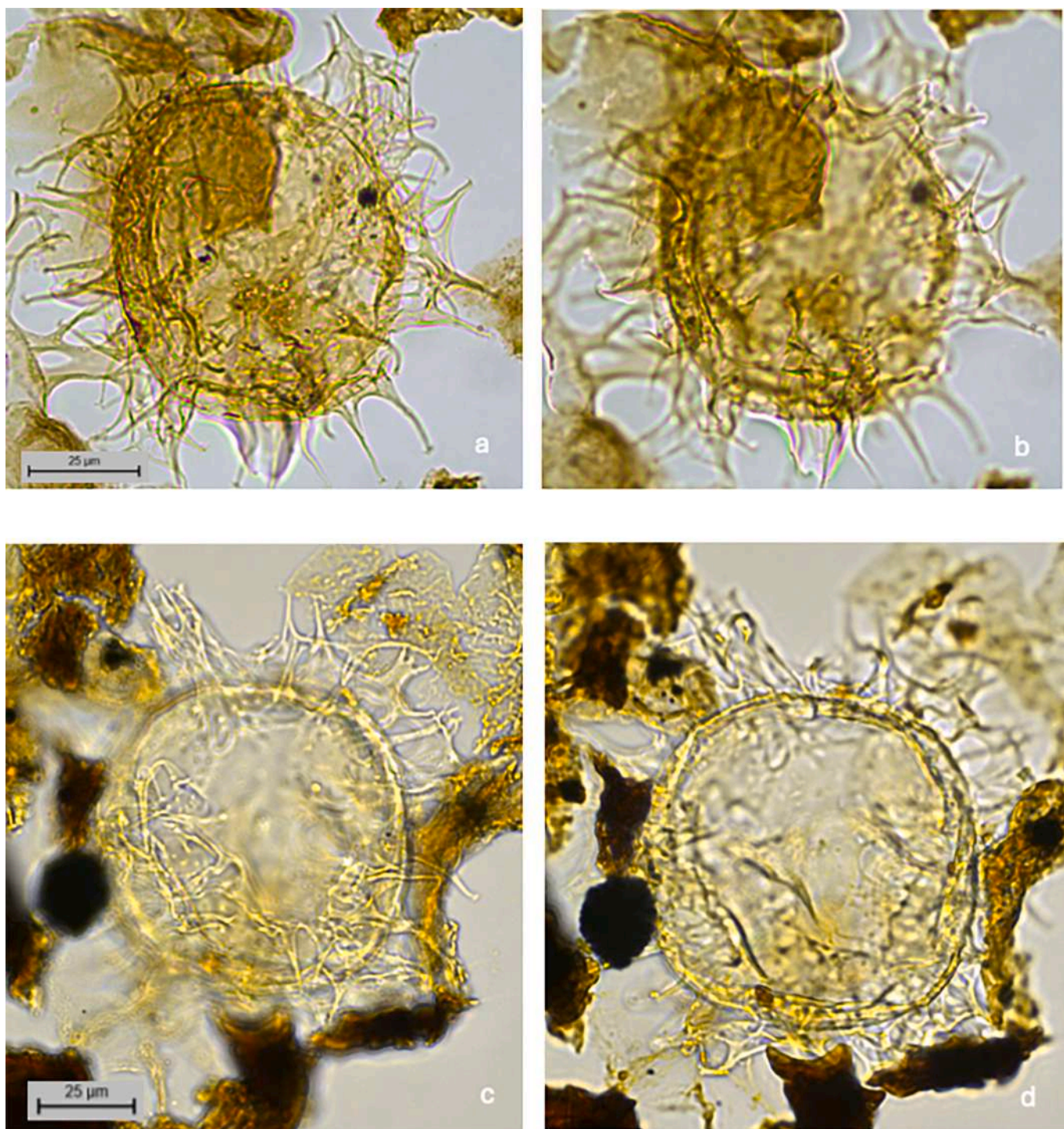


Plate III. a–b. *Explodinium priabonensis* gen. et comb. nov. high focus to low focus, from dorsal to ventral side. Sample KR22S1Y1, slide 1, EF: R29/1. c–d. *Explodinium priabonensis* gen. et comb. nov. high focus to low focus, from ventral to dorsal side. Paratype 2, sample KR22S3Y17, slide 1, EF: G19/3.

supplemental material), may well explain the rather expanded portion assigned to the overlying Rac Zone (Fig. 4). Other options for missing section include the frequently occurring small- to larger scaled faulting in the cliff sections at Karaburun (see, e.g., figs. 1c and 1d of Kaya et al., 2025, notably between subsections KR-1 and KR-3).

4. Concluding remarks

Our more focused study of the dinocyst distribution across the EOT interval of the Karaburun section, NW Turkey, yields a more detailed

picture of correlative secondary bioevents allowing a more robust correlation to the Italian type sections. Particularly the ranges of the (herein taxonomically revised) species *Explodinium priabonensis* gen. et comb. nov. and the new species *Glaphrocysta peterbijlii* sp. nov. may be regarded as additional criteria to correlate EOT strata within the Mediterranean (incl. the Paratethyan realm). Combined evidence now suggests that while the Karaburun section may not be as complete as previously assumed (cf. Kaya et al., 2025), only a very small part of the succession (part of) the Adi Zone of Brinkhuis and Biffi and the interval represented Subchron C13n to basal C13n may be missing (Figs. 3, 5). In

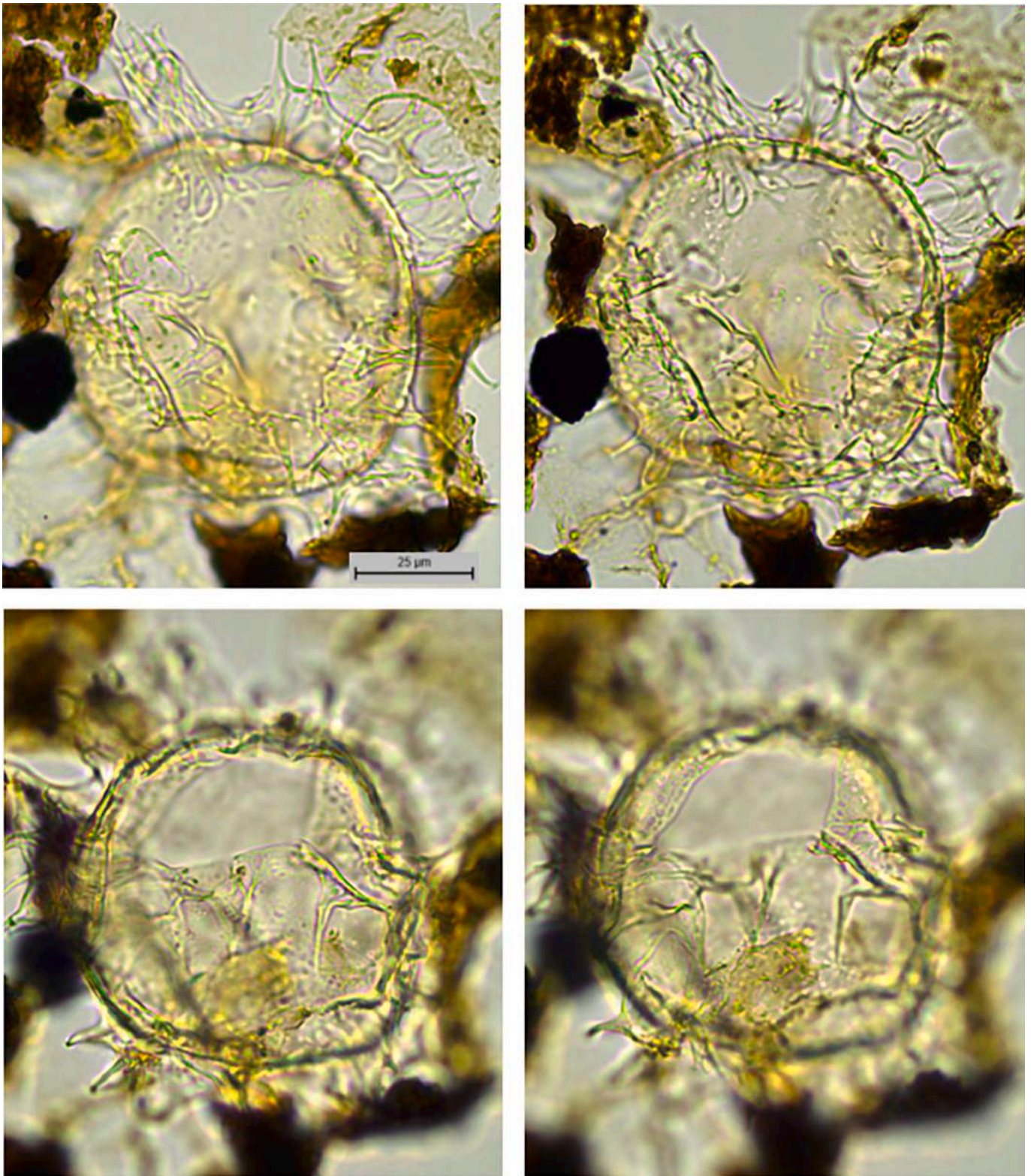


Plate IV. a–d. *Explodinium priabonensis* gen. et comb. nov., high focus to low focus, from ventral to dorsal side. Paratype 2, sample KR22S3Y17, slide 1, EF: G19/3, larger magnification than shown on the previous plate. Note the array of processes just adjacent to the archaeopyle margin, posteriorly.

view of the correlation of the position of the potential missing section to the base of the EOGM (Figs. 3, 5), a relationship to the effects of major EOT eustatic lowering and related erosion seems plausible. These results further support the general outcome and interpretations of Kaya et al. (2025).

5. Systematic paleontology

Division: DINOFAGELLATA (Bütschli, 1885) Fensome et al., 1993
Class: DINOPHYCEAE Pascher, 1914
Subclass: PERIDINIPHYCIDAE Fensome et al., 1993

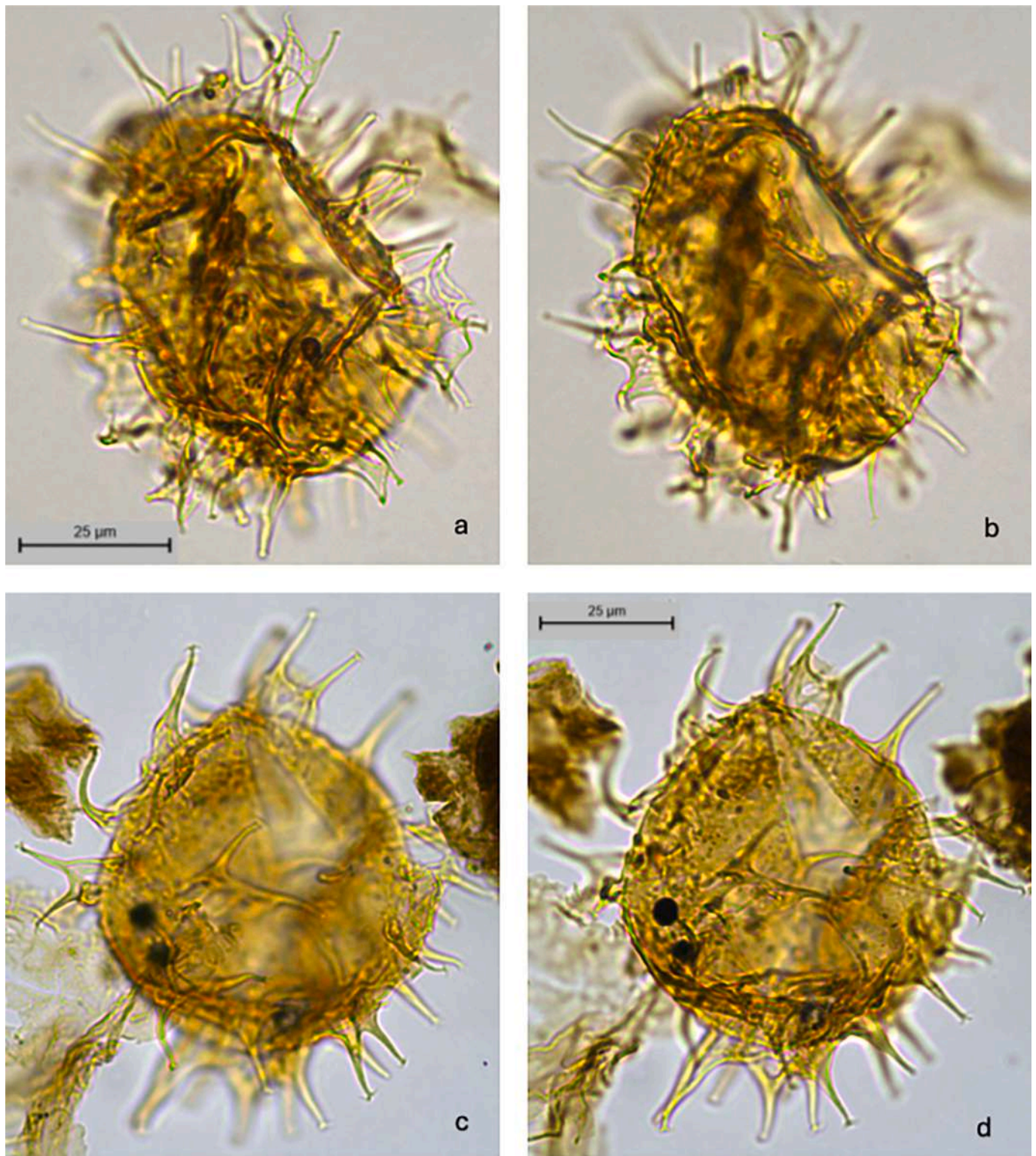


Plate V. a–b. *Explodinium priabonensis* gen. et comb. nov., high focus to low focus, from oblique ventral to dorsal side. Sample KR22S1Y16, slide 2, EF: B28/3. c–d. *Explodinium priabonensis* gen. et comb. nov., high focus to low focus from ventral to dorsal side. Sample KR22S1Y8, slide 1, EF: D25/3.

Order: GONYAULACALES Taylor, 1980

Suborder: GONYAULACINEAE (autonym)

Family: GONYAULACACEAE Lindemann, 1928

Subfamily: GONYAULACOIDEAE Fensome et al., 1993

Genus: *Explodinium* gen. nov.

Type: Brinkhuis, 1994, p. 148–149. pl. II, figs. 1–5, as '*Glaphyrocysta priabonensis*'. Restudy of the type material from the Priabona and

Bressana, and of new, better-preserved materials from Karaburun, led to the conclusion that this taxon is not characterized by an apical archaeopyle (e.g., typical for *Glaphyrocysta*), but rather by a (rather large sized) single-plate, precingular one, likely reflecting the loss of 3". This observation, and the irregularly expanded periphragm, is the basis for the erection of the new genus *Explodinium*. In addition, since, after extensive searches, we unfortunately also must conclude that the holotype of

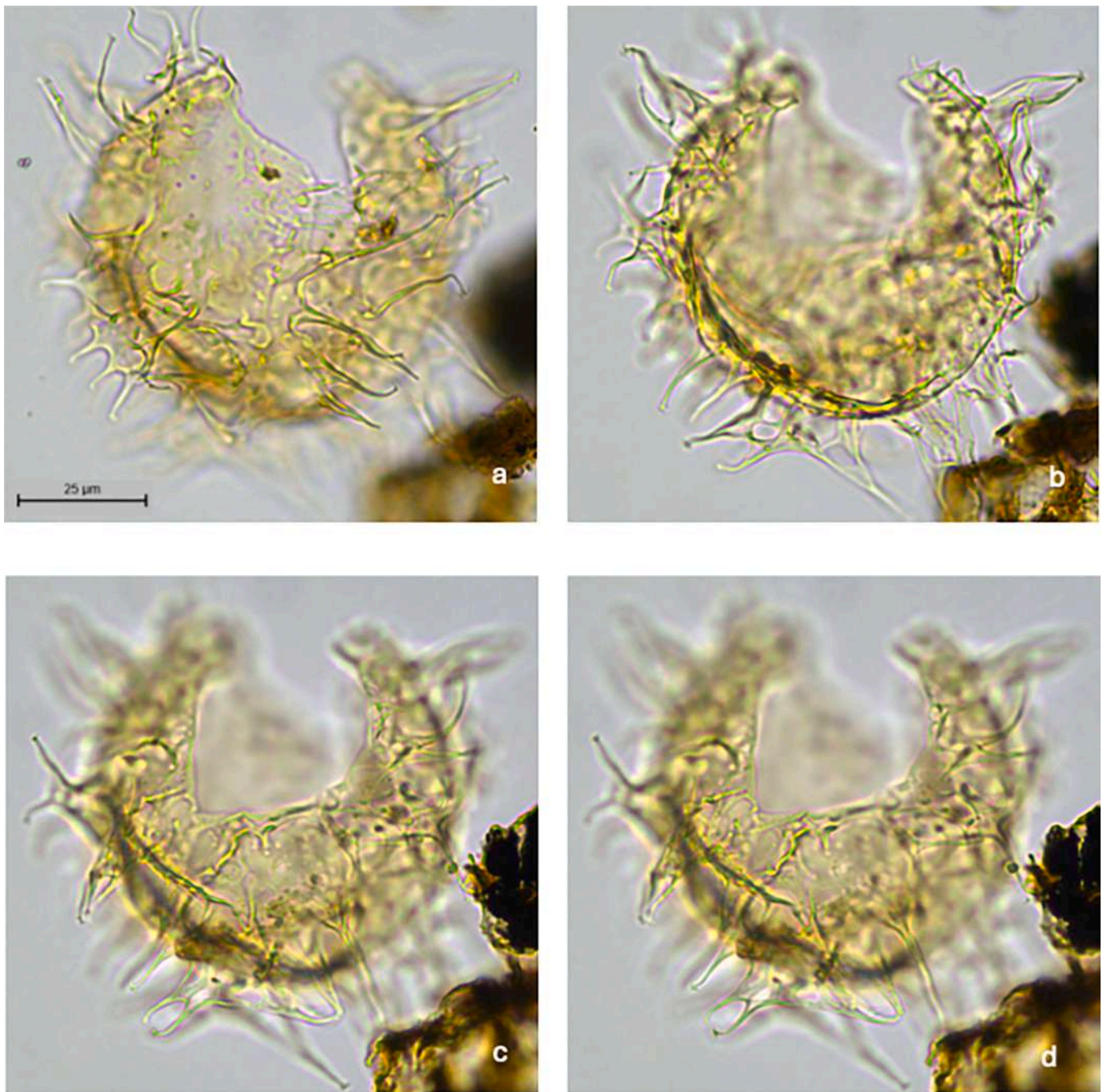


Plate VI. a–d. *Explodinium priabonensis* gen. et comb. nov., high focus to low focus, from ventral to dorsal side. Sample KR22S3Y1, slide 2, EF: D35.

'*Glaphyrocysta priabonensis*' is lost, as are most slides of the original study, we establish a **neotype** and paratypes herein, based on the Turkish material, described below, and illustrated on [Plate I](#), figs. a–f.

Etymology: Latin: *Explodere*, to explode, in reference to the typical irregularly disconnected, perforated, distally spiny periphragm relative to the subspherical endophragm, giving the appearance of an ongoing explosion.

Diagnosis: Intermediate to large-sized, ovoidal to spherical, double-walled, irregularly cavate, proximochorate cysts bearing numerous, often bifurcated spines. Outer wall (periphragm) typically finely to coarsely perforated and highly variably connected to the (smooth to scabrate) inner wall (endophragm). Typically, however, is there no, to little separation between the walls on the postcingular area likely reflecting 4'', nor are there many processes formed in that sector. The

periphragm distally forms numerous, often basally interconnected, solid-fibroid, distally closed, often bifurcated processes, with acuminate to (more typical) bifurcate tips. Archaeopyle precingular, type 1P (3''), operculum free.

Comparison: *Explodinium* gen. nov. has – besides the same archaeopyle - morphological affinities with certain reticulate to coarsely reticulated species of *Operculodinium* (e.g., *O. eisenackii*, *O. divergens*, *O. tiara*) but distinctly differs by the typical irregular (semi-) separation of the two wall layers, and the irregular distribution of processes.

Explodinium priabonensis gen. et comb. nov., emend. nov.

[Plates I–VIII](#)

1993 *Glaphyrocysta* sp. Brinkhuis and Biffi (pl. VI, figs. 5–6).

1994 *Glaphyrocysta priabonensis* Brinkhuis (pl. I, fig. 8, pl. II, figs. 1–8).

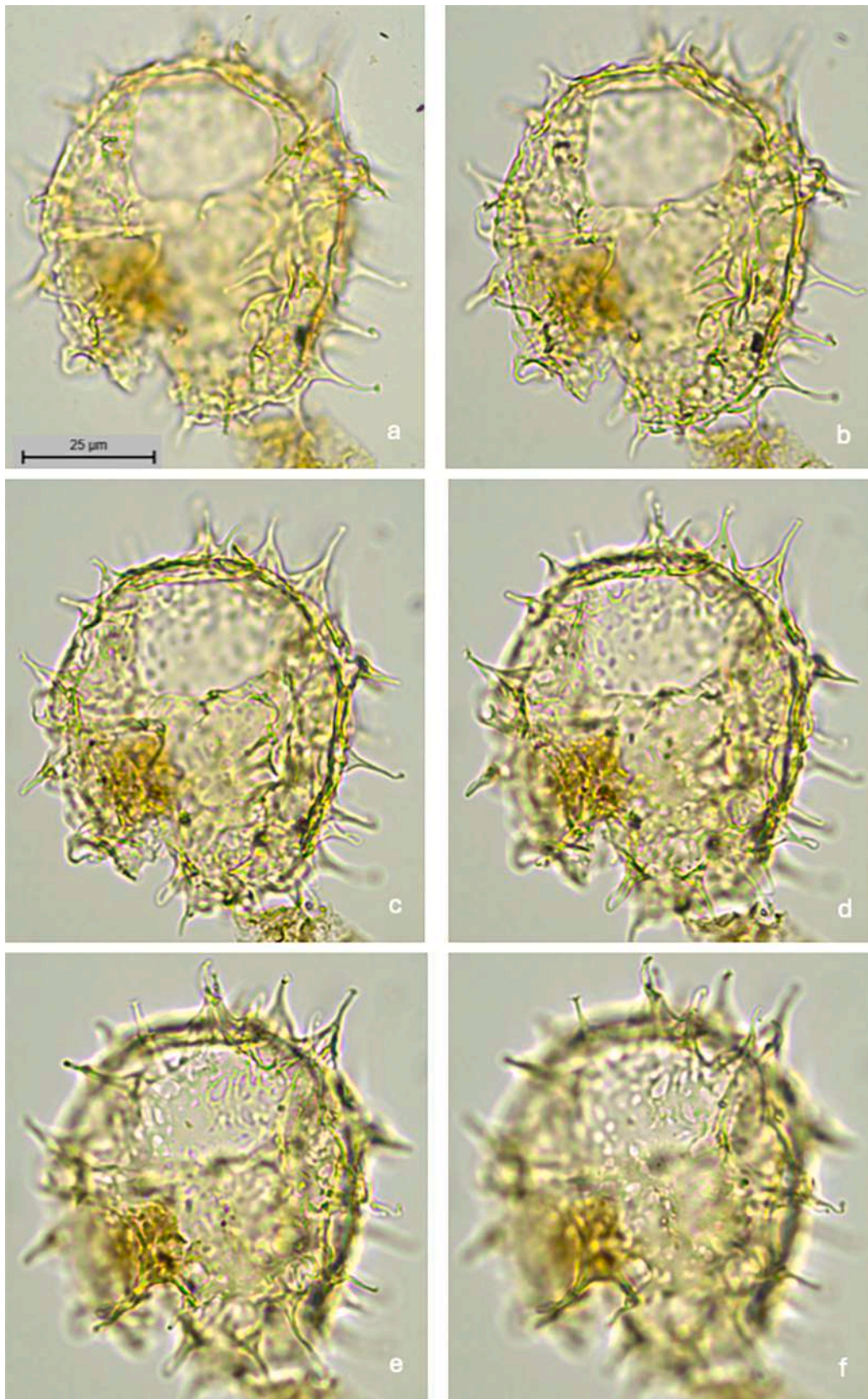


Plate VII. a–f. *Explodinium priabonensis* gen. et comb. nov., high focus to low focus, from dorsal to ventral side. Sample KR22S3Y15, slide 1, EF: G19/3.

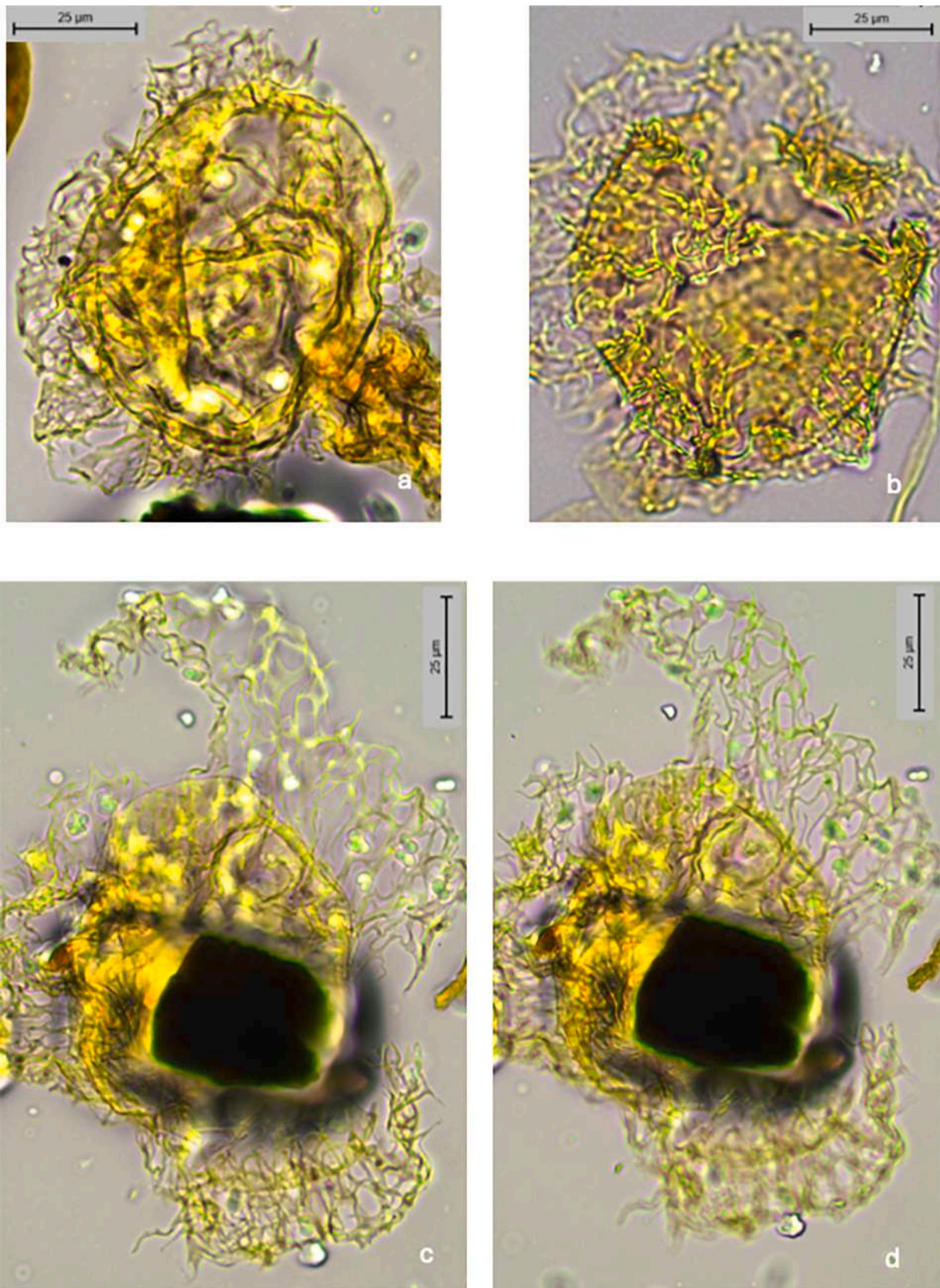


Plate VIII. Plate showing some morphological variations of poorly preserved specimens of *Explodinium priabonensis* gen. et comb. nov. from the type material, Priabona section (samples/slides from Brinkhuis, 1994, orientations unknown). a. *Explodinium priabonensis* gen. et comb. nov. Sample PB 15, slide 1, EF: O20. b. *Explodinium priabonensis* gen. et comb. nov. Sample PB 15, slide 1, EF: S22/3 c-d. *Explodinium priabonensis* gen. et comb. nov., high focus to low focus. Sample PB 15, slide 1, EF: H40/4. Note wide separation of the two wall layers.

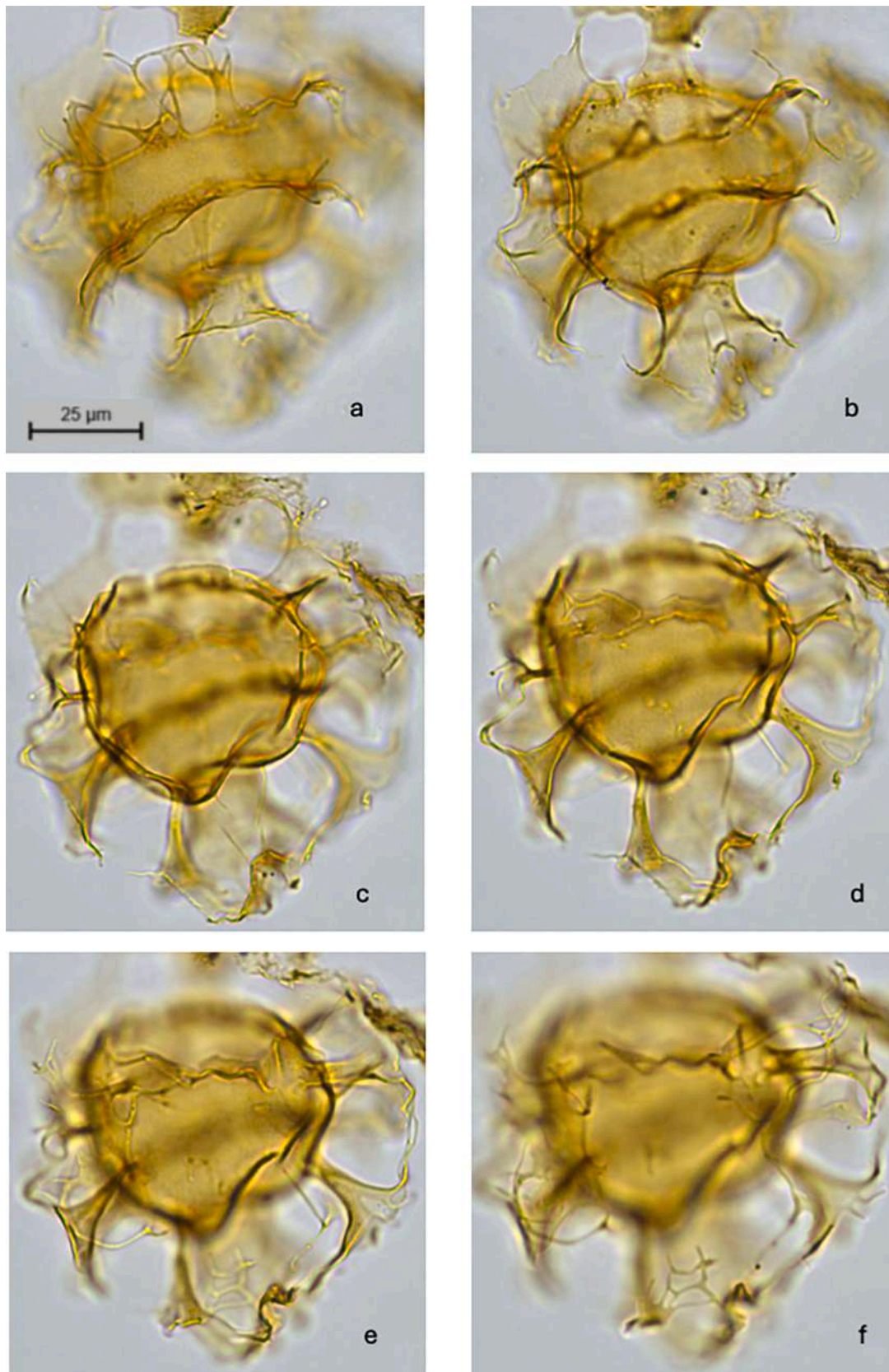


Plate IX. a–f. *Glaphyrocysta peterbijlii* sp. nov. Holotype; high focus to low focus, from dorsal to ventral side. Sample KR22S2Y23, slide 1, EF: C14. Note the complexly connected ramifications ventrally.

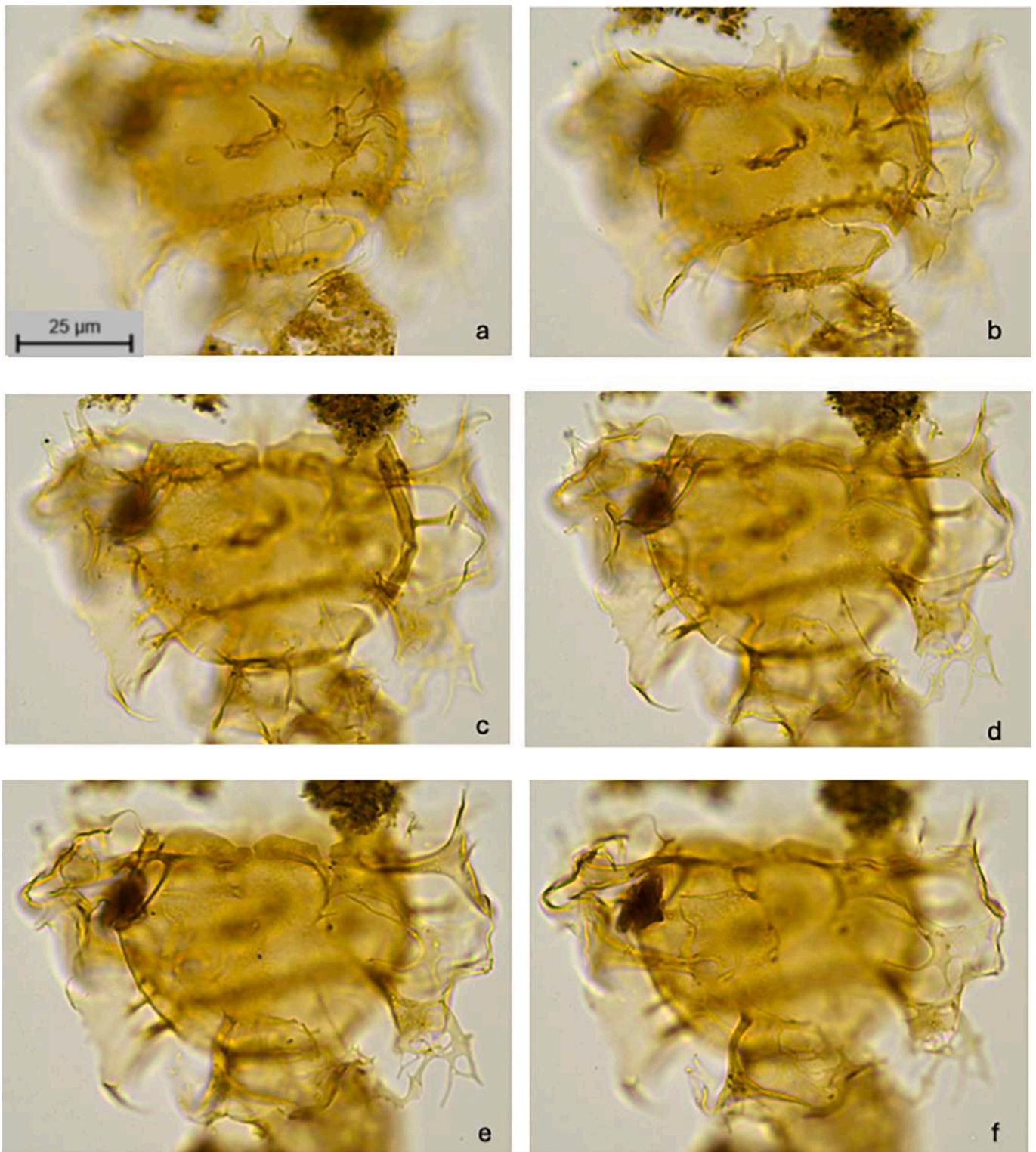


Plate X. a-f. *Glaphyrocysta peterbijlii* sp. nov. Paratype 1; No high focus to low focus, from dorsal to ventral side. Sample KR22S2Y23, slide 1, EF: R19. Note the complexly connected ramifications ventrally.

2015 *Glaphyrocysta priabonensis* Bati (pl. IX, fig. 6).

2025 *Glaphyrocysta priabonensis* Kaya et al. (SI: pl. 4, fig. g).

Remarks: This case may be taken as a good example of the proverbial ‘Murphy’s Law’. As it turns out now, and indicated already above, anno 2025, based on much better-preserved material from the Karaburun section, NW Turkey, relative to the material from central and NE Italy, including the Type Priabonian, the original diagnosis of this species by

Brinkhuis and Biffi (1993) and, more significantly, Brinkhuis (1994) is flawed. Moreover, on top of that, and unfortunately, the holotype must be regarded as lost. We therefore establish a neotype (and paratypes) herein and provide a more detailed (emended) description of the species, including its quite extensive morphological variability.

In hindsight, apparently impressed by the rather large archaeopyle, combined with the occasionally widely separated wall layers, Brinkhuis

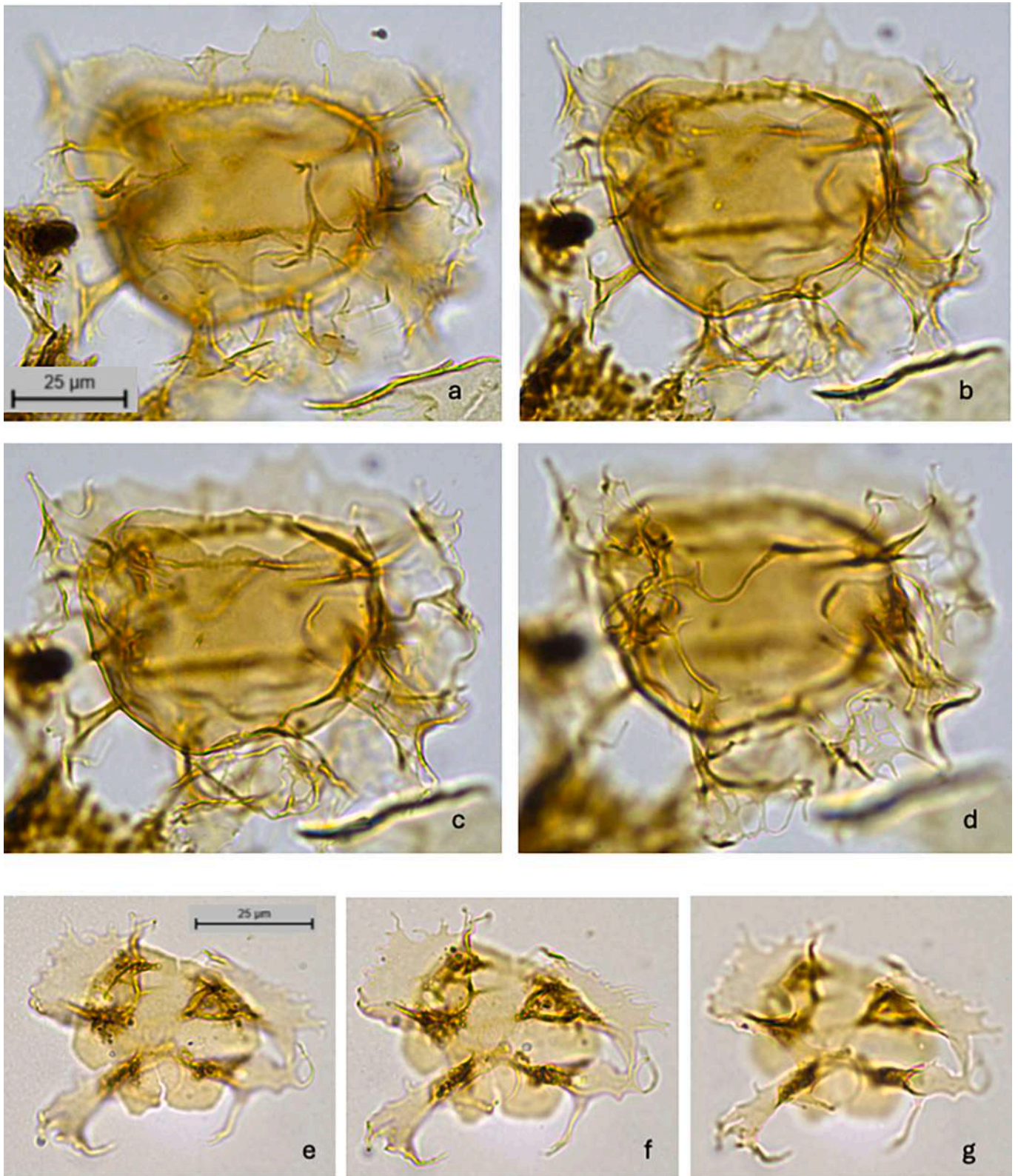


Plate XI. a–d. *Glaphyrocysta peterbijlii* sp. nov., high focus to low focus, from dorsal to ventral side. Sample KR22S2Y23, slide 1, EF: C26. e–g. *Glaphyrocysta peterbijlii* sp. nov., operculum, high focus to low focus. Sample KR22S2Y23, slide 1, EF: C22/3. Note the larger 2' and 3' relative to the 1' and 4'.

(1994) surmised an apical archaeopyle, and from there, interpreted the irregular, but in the case of the holotype, widely separated wall layers as indicative for a morphological relationship to *Glaphyrocysta* species (e. g., Brinkhuis, 1994, fig. 16). The unusual situation of having compressed walls (and thus absence of cavation) in the area what is here

reinterpreted as the dorsal side, added back then to the notion that it concerned a new species of *Glaphyrocysta*. Indeed, the better-preserved specimens from Karaburun (see pls. I–VII) now allow for a much clearer picture of the peculiar morphology and large morphological variability of this species, both in terms of size as well as in degree of

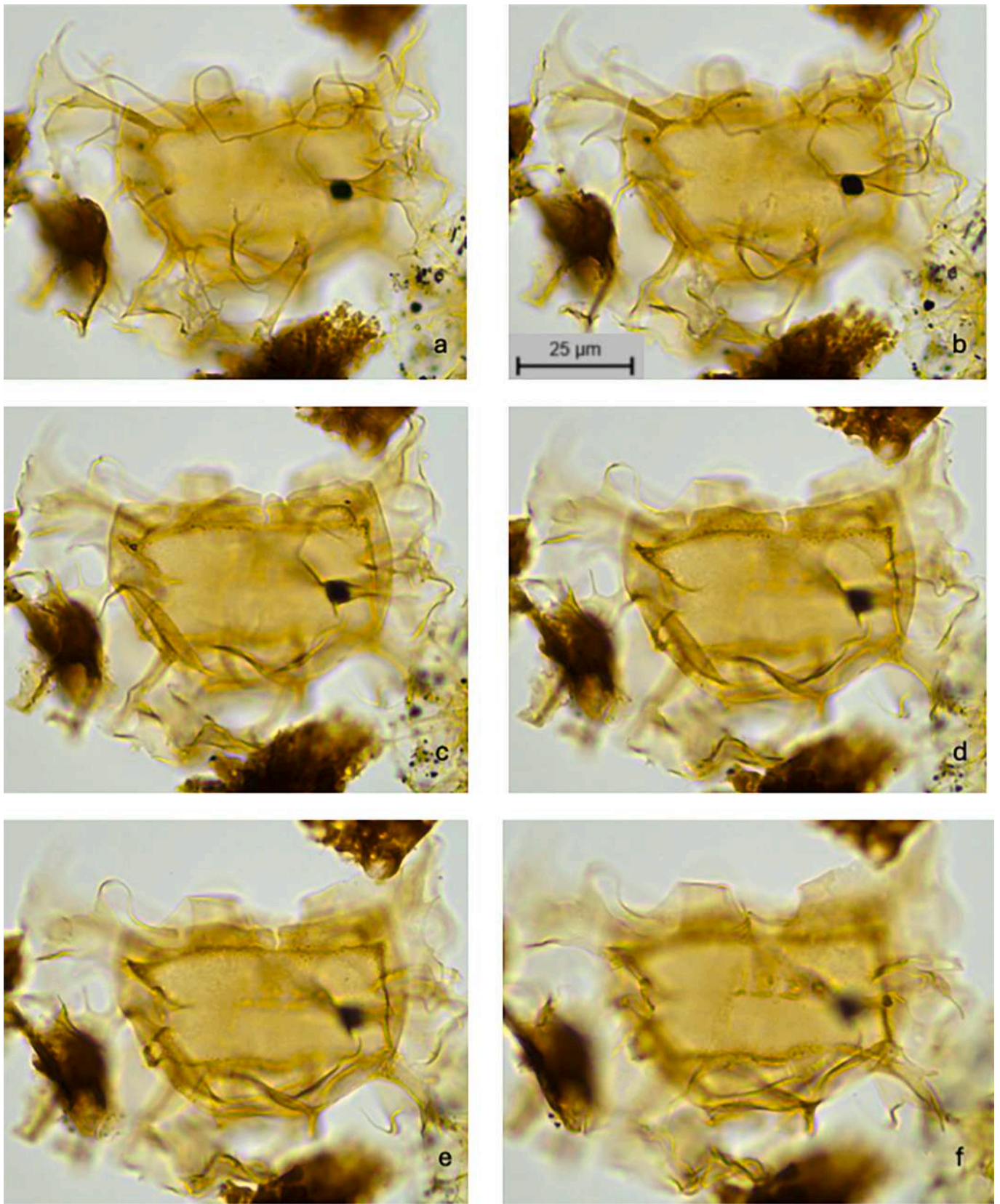


Plate XII. a–f. *Glaphrocysta peterbijlii* sp. nov., high focus to low focus, from ventral to dorsal side. Paratype 2; sample KR22S2Y29, slide 2, EF: R29/1.

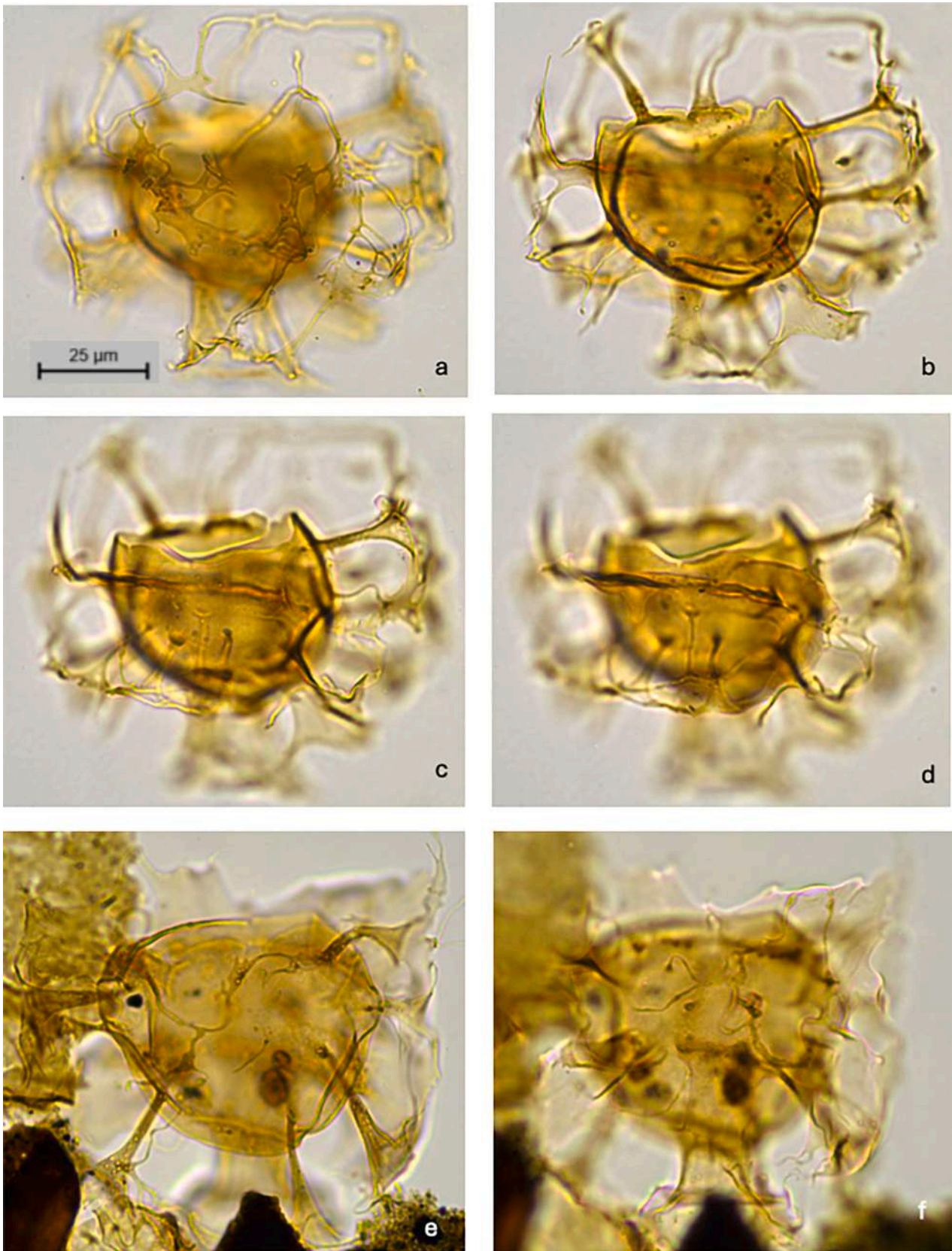


Plate XIII. a–d. *Glaphrocysta peterbijlii* sp. nov., high focus to low focus, from ventral to dorsal side. Sample KR22S2Y23, slide 1, EF: C47/4. Note the complexly connected ramifications ventrally. e–f. *Glaphrocysta peterbijlii* sp. nov., high focus to low focus, from ventral to dorsal side. Sample KR22S2Y23, slide 1, EF: G29.

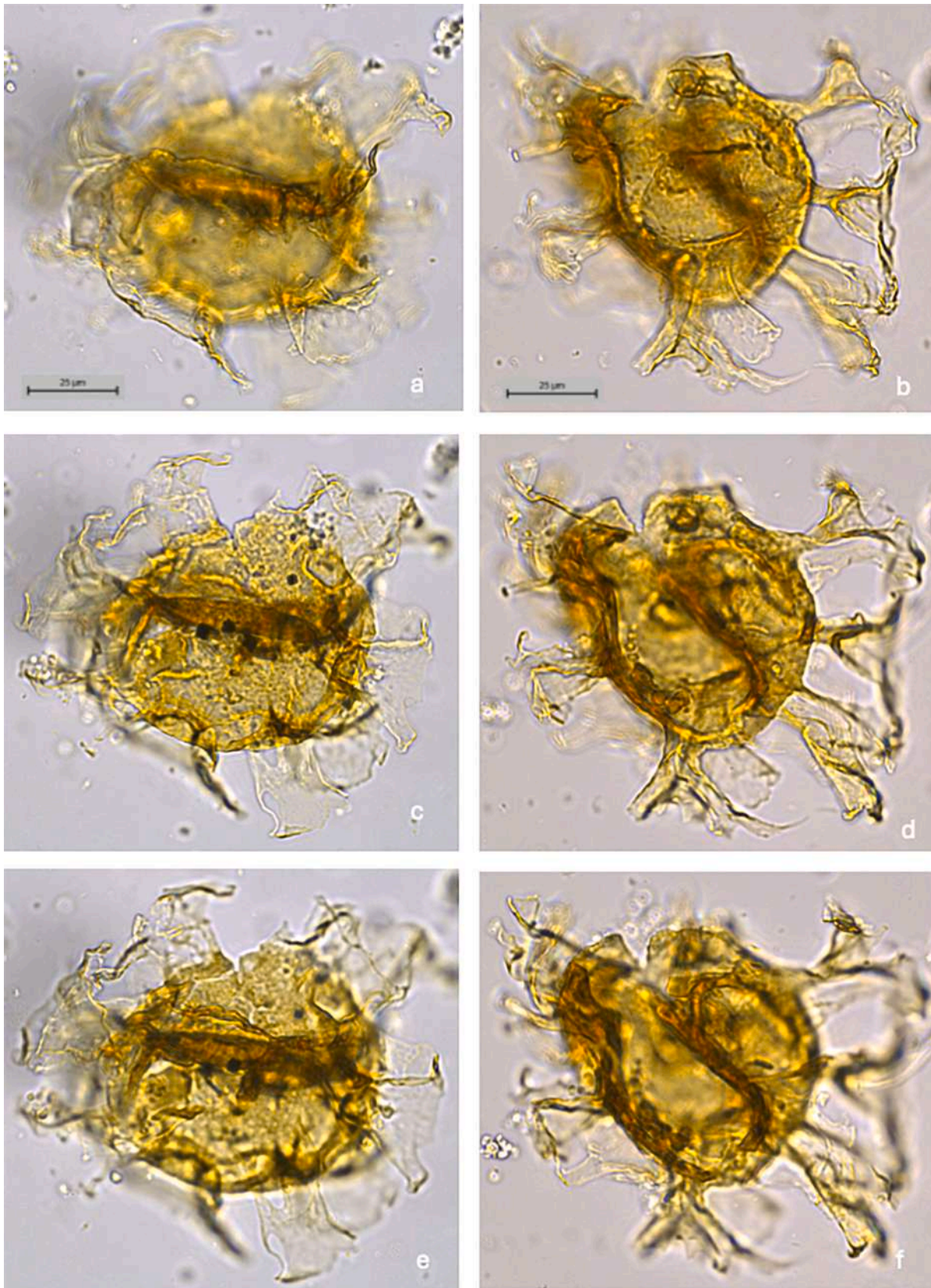


Plate XIV. Plate showing some morphological variations of poorly preserved specimens of *Glaphyrocysta peterbijlii* sp. nov. from the type Priabonian, Bressana section (samples/slides from Brinkhuis, 1994, therein identified as '*Areoligera sentosa*'). a, c, e. *Glaphyrocysta peterbijlii* sp. nov., high focus to low focus, from dorsal to ventral side. Sample BS44 (Brinkhuis, 1994), slide 1, EF: F35. b, d, f. *Glaphyrocysta peterbijlii* sp. nov., high focus to low focus, from dorsal to ventral side. Sample BS44 (Brinkhuis, 1994), slide 1, EF: F35/3.

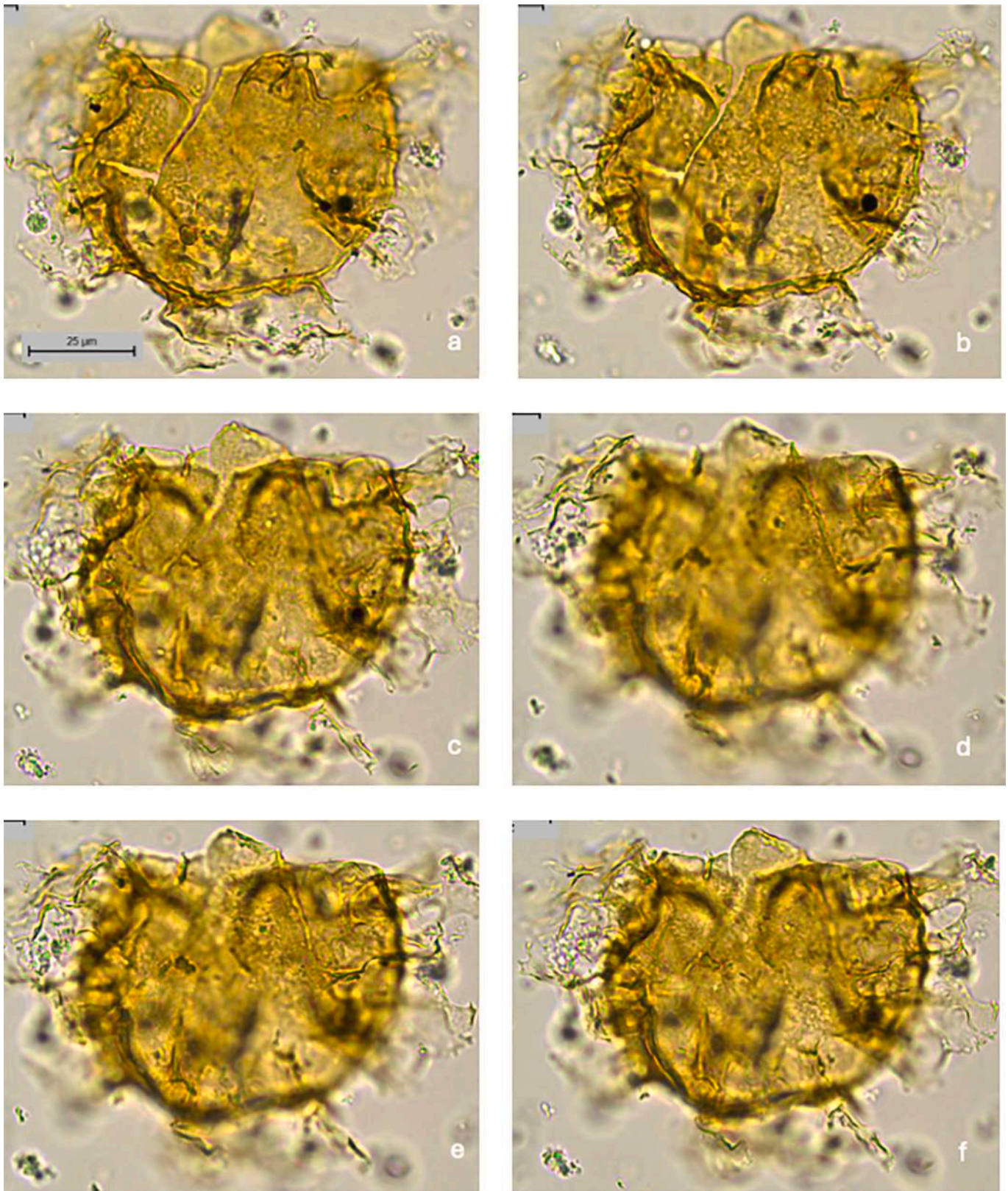


Plate XV. Plate showing a poorly preserved specimen of *Glaphyrocysta peterbijlii* sp. nov. from the type Priabonian, Bressana section (samples/slides from [Brinkhuis, 1994](#), therein identified as '*Areoligera undulata*'). a-f. *Glaphyrocysta peterbijlii* sp. nov., high focus to low focus, from dorsal to ventral side. Sample BS44 ([Brinkhuis, 1994](#)), slide 1, EF: N43/2.

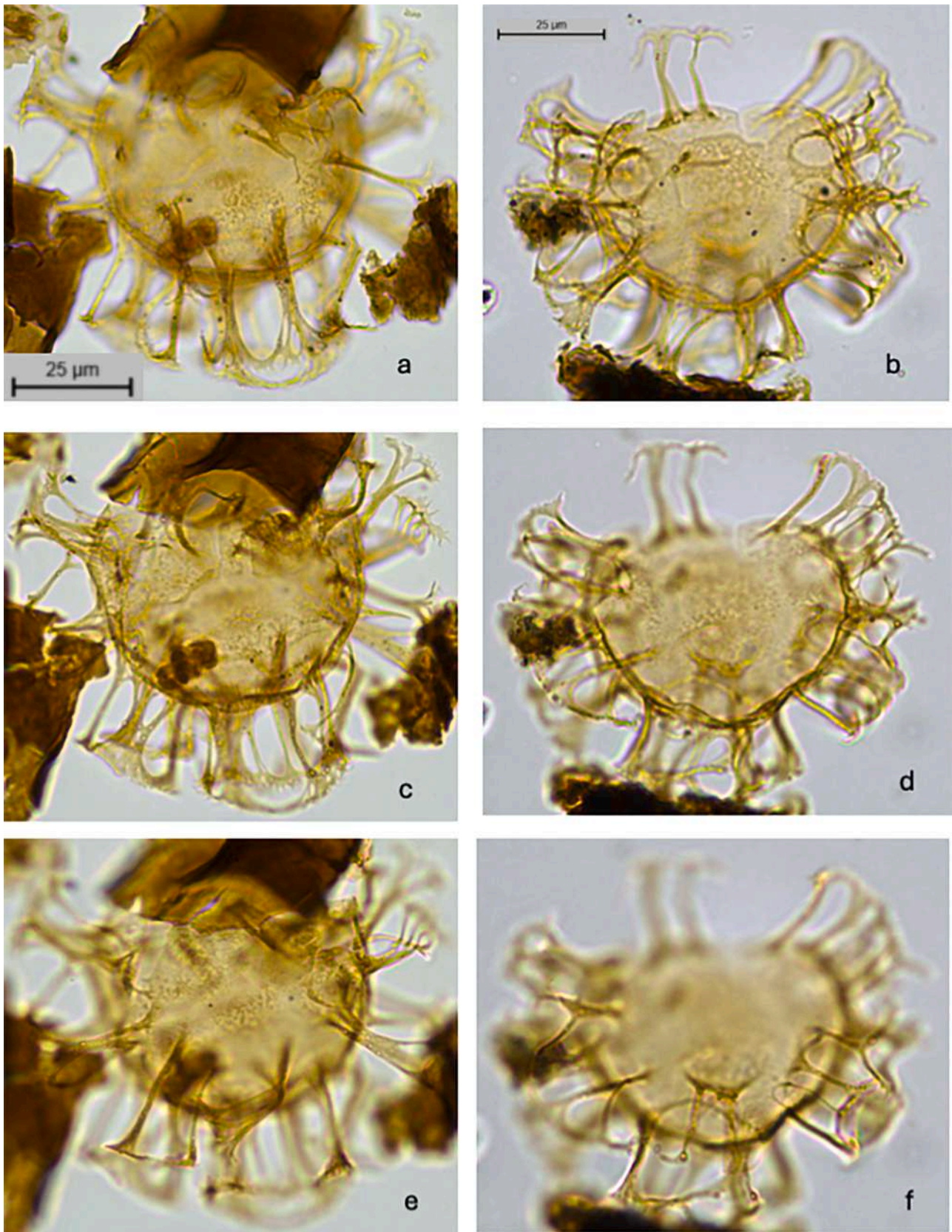


Plate XVI. Plate showing some morphological variations within *Glaphyrocysta intricata* from the Karaburun section. Also added here to illustrate the similarities between the successive genera established within the Areoligeraceans. Not that this species has no, or minute distal connections between the process-clusters. a, c, e. *Glaphyrocysta intricata*, high focus to low focus, from dorsal to ventral side. Sample KR22S1Y8, slide 2, EF: G25/3. b, d, f. *Glaphyrocysta intricata*, high focus to low focus, from dorsal to ventral side. Sample KR22S2Y40, slide 1, EF: O42.

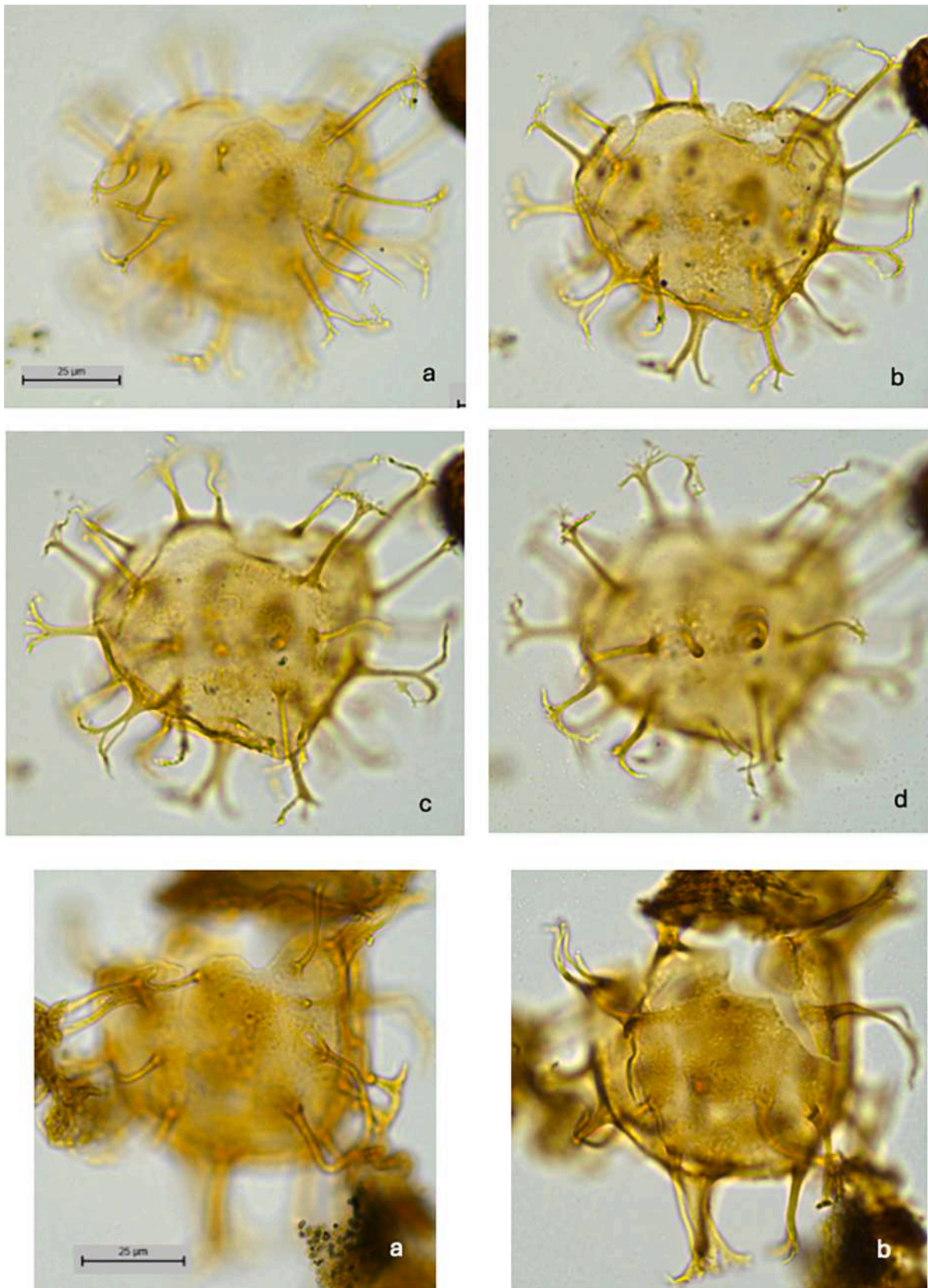


Plate XVII. a–d. *Licracysta corymbus*, high focus to low focus, from ventral to dorsal side. Sample KR22S2Y45, slide 1, EF: D15. e–g. *Licracysta corymbus*, high focus to low focus, from ventral to dorsal side. Sample KR22S2Y45, slide 1, EF: C26/4.

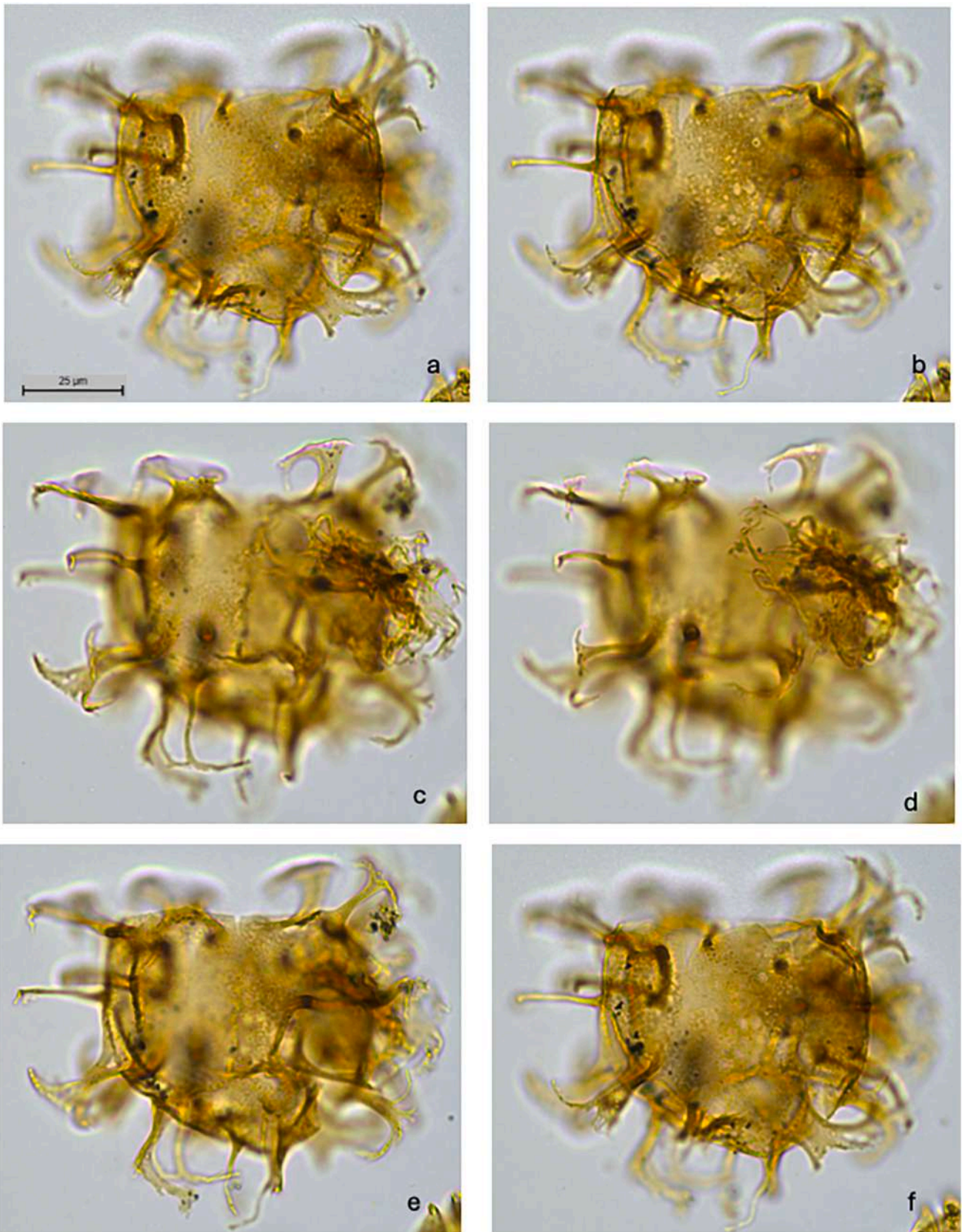


Plate XVIII. a-f. *Licracysta? semicirculata* high focus to low focus, from oblique dorsal to ventral side. Sample KR22S2Y45, slide 1. EF: R43-2.

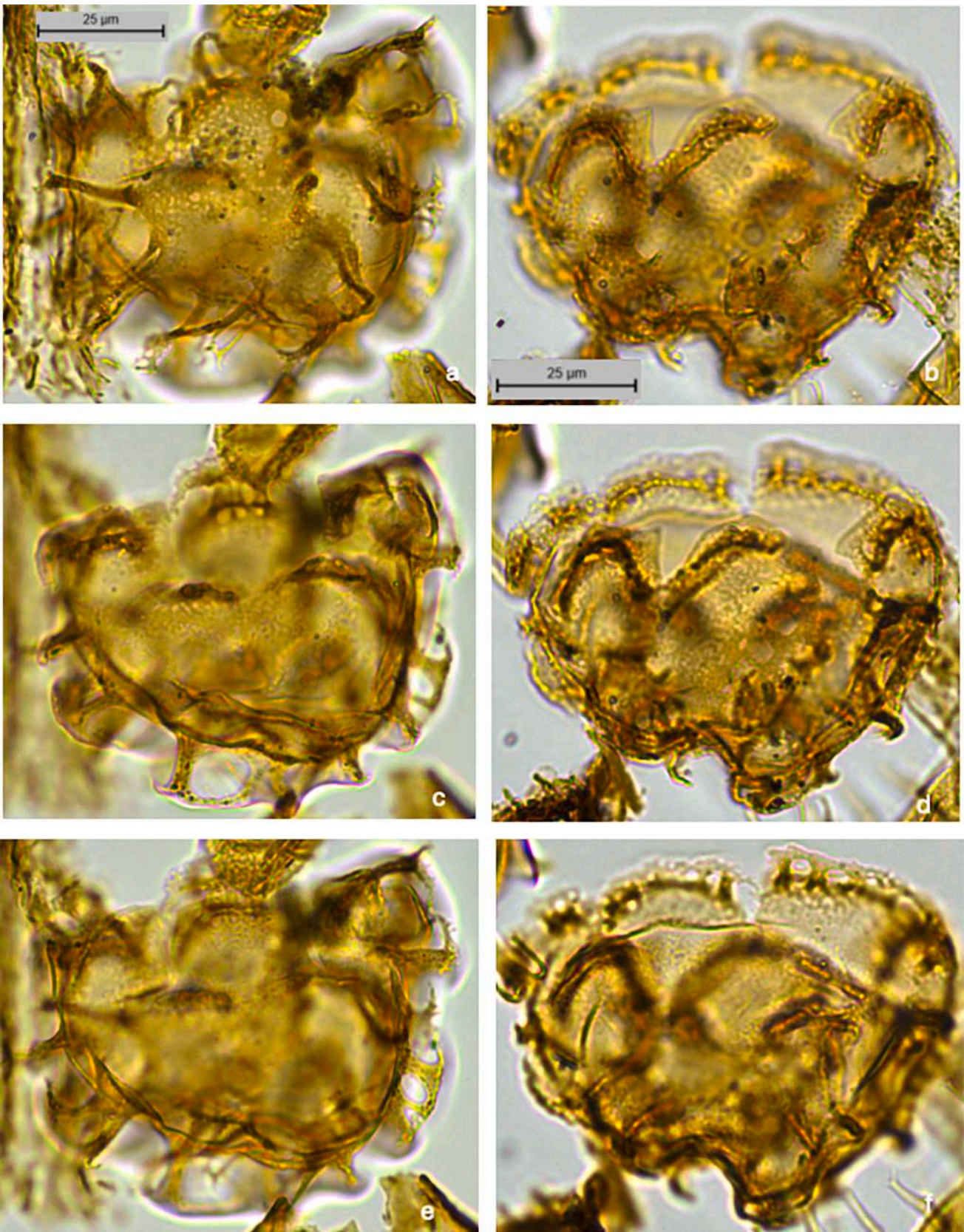


Plate XIX. Plate showing some morphological variations within *Licracysta? semicirculata* from the Karaburun section. a, c, e. *Licracysta? semicirculata*, high focus to low focus, from ventral to dorsal side. Sample KR22S2Y45, slide 1, EF: K24/4.
 b, d, f. *Licracysta? semicirculata*, high focus to low focus, from dorsal to ventral side. Sample KR22S2Y45, slide 1, EF: G28/3.

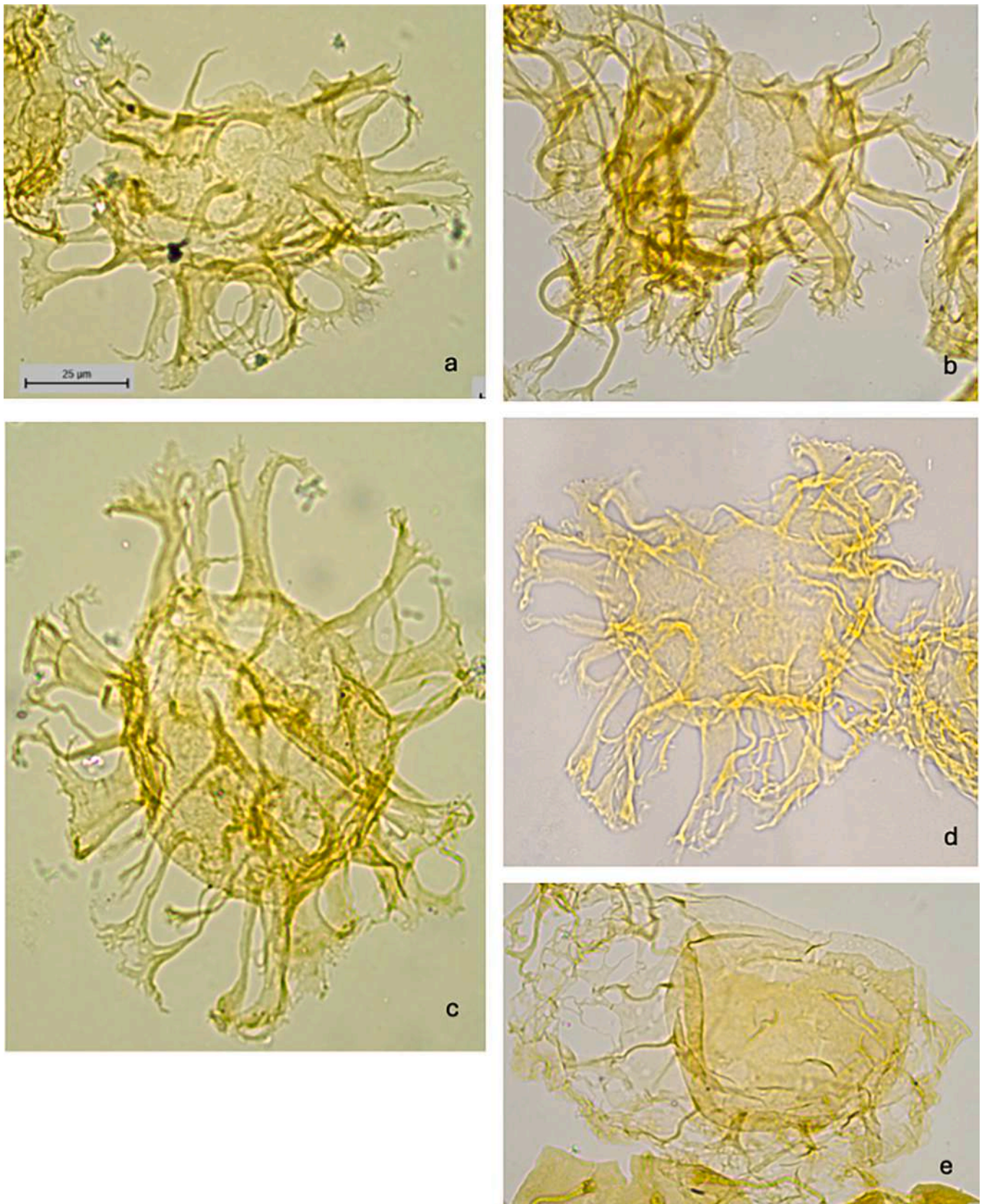


Plate XX. Plate showing some poorly preserved Areoligeraceans from the top part of the Priabonian Type section (samples/slides from [Brinkhuis, 1994](#)). a. *Licracysta corymbus* (?), ventral view. Sample PB28 ([Brinkhuis, 1994](#)), slide 1, EF: H31/4. b. *Licracysta corymbus* (?) ventral view. Sample PB28 ([Brinkhuis, 1994](#)), slide 1, EF: H32/3. c. *Licracysta? semicirculata*, (?) ventral view (?). Sample PB28 ([Brinkhuis, 1994](#)), slide 1, EF: P36. d. *Glaphyrocysta intricata* (?), ventral view. Sample PB28 ([Brinkhuis, 1994](#)), slide 1, EF: H40/4. e. *Glaphyrocysta semitecta*, ventral view. Sample PB28 ([Brinkhuis, 1994](#)), slide 1, EF: J35.

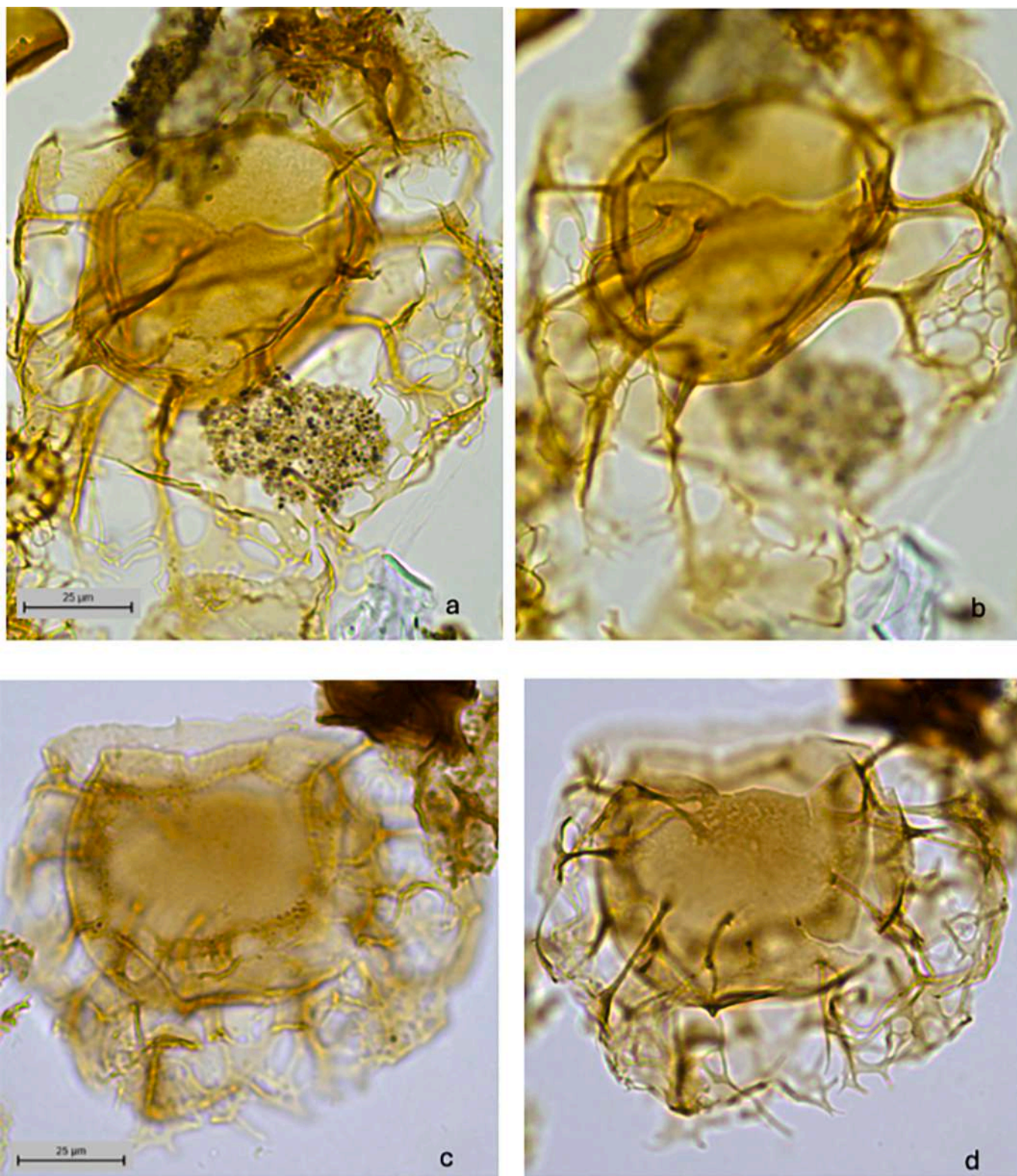


Plate XXI. a–b. *Glaphyrocysta semitecta*, high focus to low focus, from mid focus to ventral side. Sample KR22S2Y41, slide 1, EF: Y41. c–d. *Glaphyrocysta semitecta*, high focus to low focus, from mid focus to ventral side. Sample KR22S2Y1, slide 2, EF: C31/4.

cavation.

(*Neo*)Type locality and horizon: Sample A5969, level 59,69 m, Karaburun section, Turkey (cf. Kaya et al., 2025).

(*Neo*)Type and paratypes: As noted above, the holotype as figured in Brinkhuis (1994) is lost, and hence a neotype is established here, viz., neotype: Plate I, figs. a–f., sample KR22-S1Y8, slide 2, EF: K42; lodged at

Utrecht University, The Netherlands. Further, Brinkhuis (1994) did not assign any paratypes, but we do so herein, viz.: Paratype 1: Plate II, figs. a. f., sample KR22-S1-Y10, slide 1, EF: O9. Paratype 2: Plate III, figs. c–d., and Plate IV, figs. a–d., sample KR22-S3-Y17, slide 1, EF: G19/3, all lodged at Utrecht University, The Netherlands.

Studied material: Karaburun section, Turkey (cf. Kaya et al., 2025),

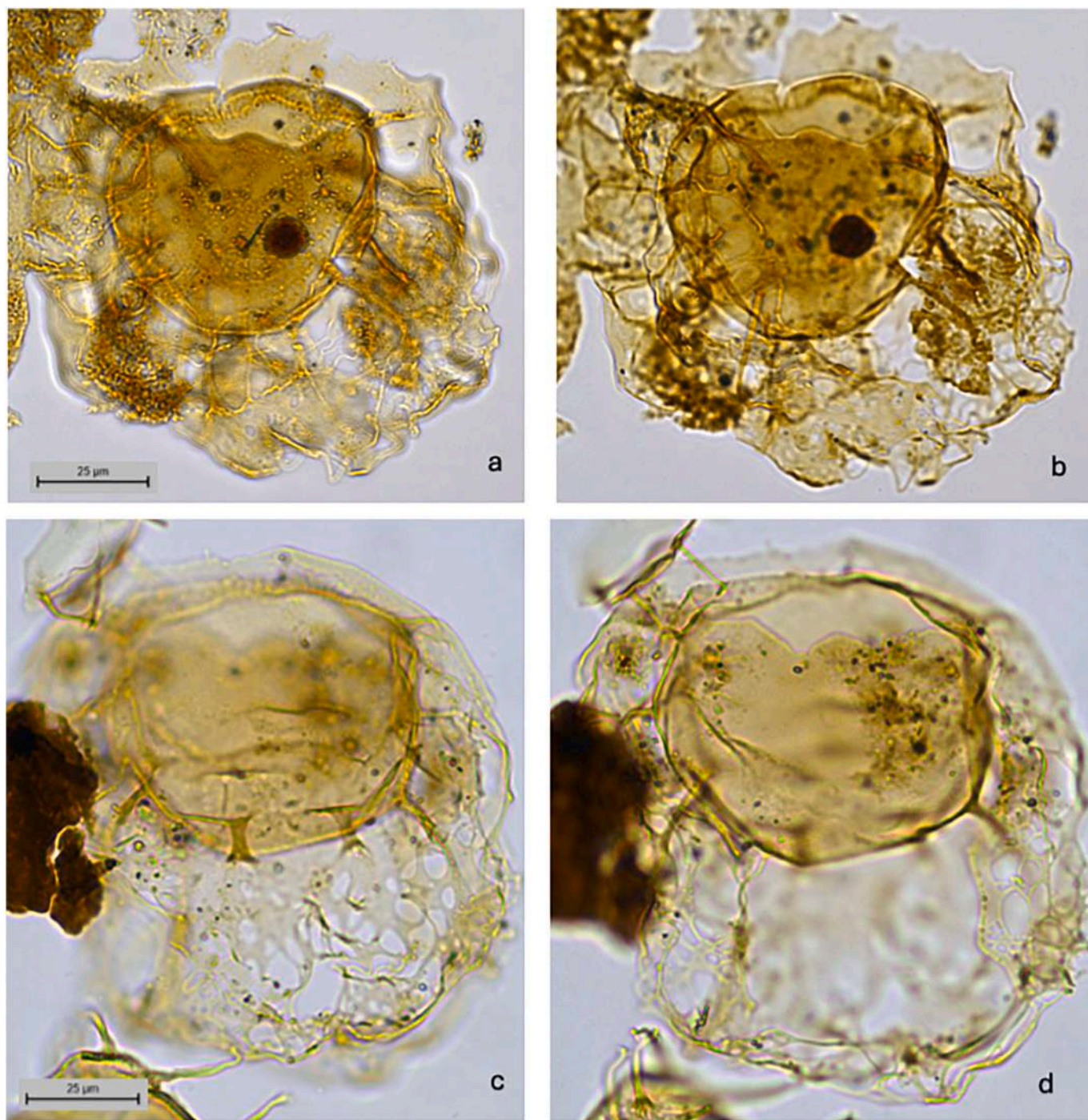


Plate XXII. a–b. *Glaphyrocysta semitecta*, high focus to low focus, from mid focus to ventral side. Sample KR22S2Y14, slide 1, EF: V24–1. c–d. *Glaphyrocysta semitecta*, high focus to low focus, from mid focus to ventral side. Sample KR22S2Y11, slide 1, EF: X14.

and the Priabona and Bressana sections from Italy (cf. Brinkhuis, 1994). Neotype and paratypes are from the İhsaniye Formation, Karaburun section, subsections KR22-S1 and KR22-S3 of Kaya et al., 2025 (samples KR22-S1-Y8 through KR22-S3-Y17).

Emended diagnosis: An intermediate to large sized species of *Explo-dinium*, bearing numerous, often basally to mid-length interconnected, solid-fibroid, distally closed, processes with acuminate to (more typical) bifurcate tips. Typically, no, to little separation occurs between the two walls on the postcingular area likely reflecting 4" (i.e. mid-dorsally, symmetrical to 3"), nor are there many processes formed in that sector (i.e., giving a 'camo-cavate' impression). This while the cingular-portion

adjacent to the archaeopyle margin seems to be reflected by a set of small spines 'per cingular plate area' (see e.g., Plate I, figs. e–f., Plate II, figs. e. f.). The wall-separation is highly irregular, as is the degree of cavation, ranging from a few μm to tens of μm .

Emended description:

Shape: Endophragm: Ovoidal. Periphragm: spiny, highly irregular in outline, processes basally to mid-process irregularly connected, with mostly bifurcate terminations.

Wall relationships: The endophragm is except for the middorsal area irregularly overlain by an often perforated, sometimes alveolate periphragm, irregularly disconnecting and giving rise to numerous spiny

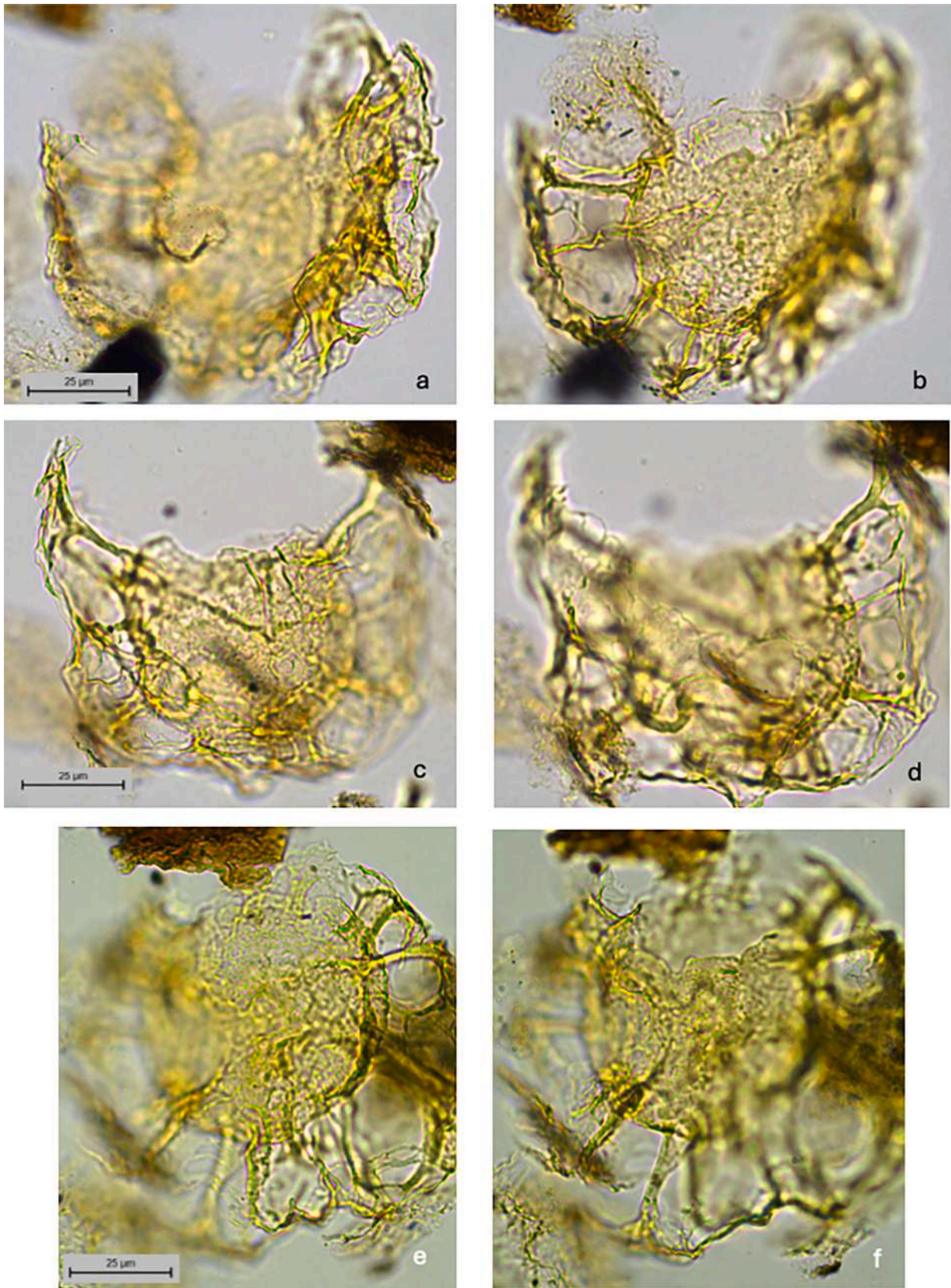


Plate XXIII. Plate showing a selection of specimens assigned to *Glaphyrocysta semitecta* (high focus to low focus) from the Bartonian/Priabonian GSSP section at Alano, NE Italy (cf. [Iakovleva, 2025](#); Houben et al., in prep.). Note the rather coarse granulated structure of the periphragm when appressed to the endophragm (notably the mid ventral area). Pictures courtesy of Alina Iakovleva, and from Houben et al., in prep.).

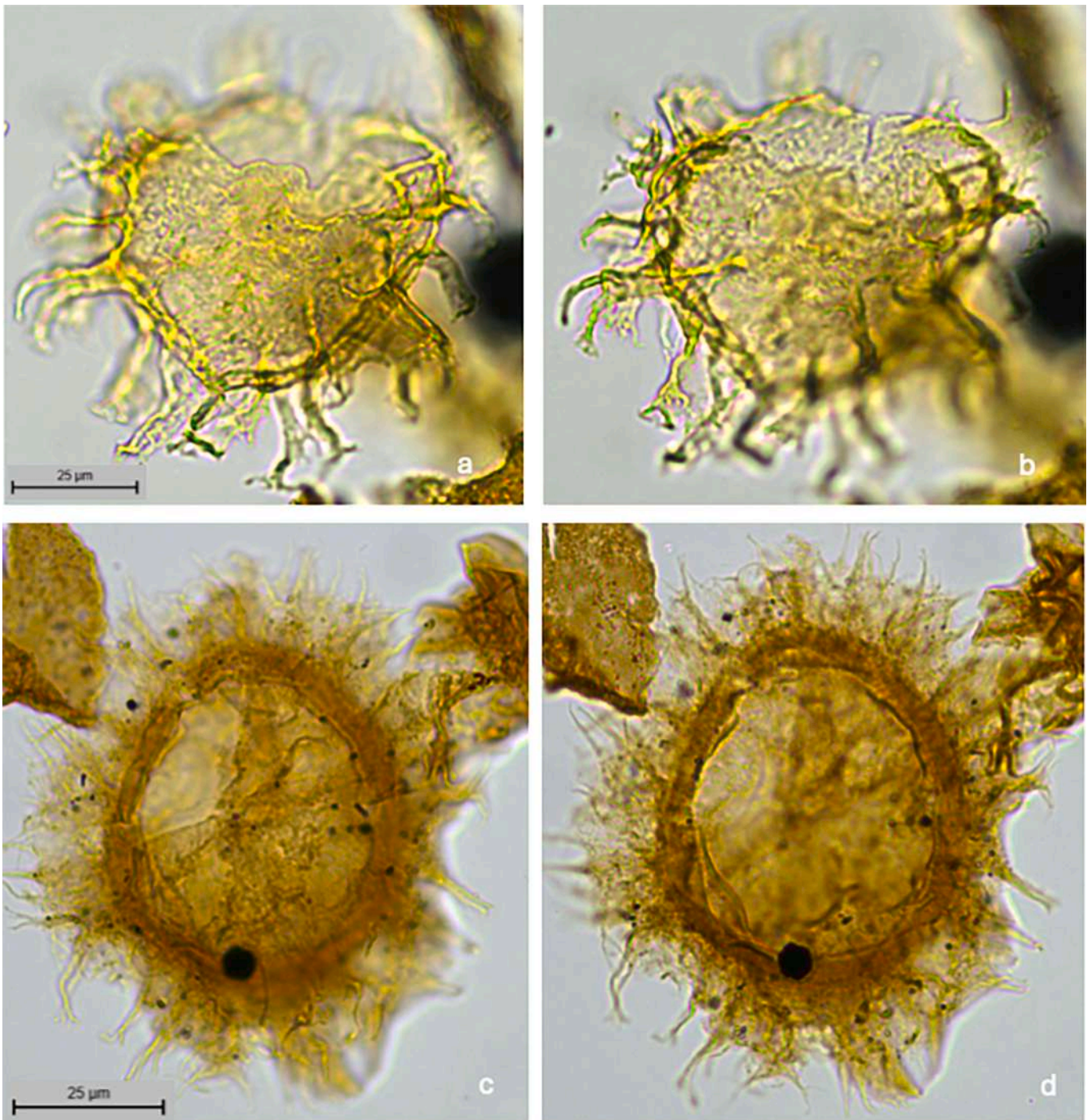


Plate XXIV. a–b. A specimen tentatively assigned to *Licracysta* sp. from the Bartonian/Priabonian GSSP section at Alano, NE Italy (see [Iakovleva, 2025](#); pictures from Houben et al., in prep.). High to low focus, from ventral to dorsal side. c–d. *Operculodinium* cf. *hirsutum*, Sample KR22S2Y14, slide 1, EF: N26/4. High to low focus, from dorsal to mid focus. Note archaeopyle indicating the loss of 3'.

processes, mostly distally bifurcated.

Wall features: Endophragm smooth, or scabrate to microgranulated, overlain by an irregularly disconnecting periphragm giving rise to numerous spiny processes, or complexes.

Processes: These are typically basally to mid-process irregularly connected, with mostly bifurcate terminations, typically occurring in sets of two (somewhat resembling giving a 'V' or 'victory' sign with your fingers). In extreme cases, the periphragm is widely separated from the endophragm and processes may be very short (aculeate to bifurcate) in those cases (compare e.g., the illustrations of [Brinkhuis \(1994\)](#), notably

pl. II, figs. 1–5, and [Plate VIII](#) herein, all from the type Priabonian sections).

Paratabulation: Indicated by the archaeopyle only, plus perhaps some (para) cingular features (sets of small processes) on the dorsal side, below the archaeopyle margin. Tabulation likely standard (neutral torsion) Gonyaulacean; likely formula 4', 5–6'', 5c?, 5'', 1p, 1''''.

Archeopyle: Precingular, type P (paraplate 3''), operculum free.

Dimensions: Central body length: 40–77 µm (neotype, 62 µm); width: 35–75 µm (neotype, 63 µm). Overall length/width: 65–115 µm (neotype, 80–90 µm). Thirty-five specimens were measured.

Stratigraphic range: Upper Priabonian (consistent) to lowermost Rupelian (isolated specimens).

Comparison: The morphology of *Explodinium priabonense* gen. nov. and nov. comb. is quite unique. Some middle to late Eocene forms that e. g., Heilmann-Clausen and Van Simaey (2005, pl. 2, fig. 12) assigned to ‘*Cordosphaeridium* aff. *callosum*’ from the Danish Basin, and/or those that are assigned to ‘*Lanternosphaeridium lanosum*’ by Iakovleva et al. (2024, pl. 11, fig. 9) from Armenia appear somewhat similar, but lack the detached periphragm, and are much more fibrous in nature. Specimens close to these morphotypes also occur in the present material, and are assigned to *Operculodinium* cf. *hirsutum*, (Plate XXIV, figs. c–d) but are quite rare and much longer ranging.

Family: AREOLIGERACEAE Evitt 1963b

Genus: *Glaphyrocysta* Stover and Evitt, 1978

Glaphyrocysta peterbijlii sp. nov.

Plates IX–XV

2015 ‘? *Areoligera sentosa-tauloma*’ Bati, pl. X, figs. 10–11.

2025 *Glaphyrocysta* sp. A. Kaya, et al. (supplemental information; dinocyst distribution chart).

Etymology: Named for Dr. Peter K. Bijl, in recognition of his achievements in marine palynology at the Marine Palynology and Paleocyanography group (MPP), Laboratory of Palaeobotany and Palynology, Department of Earth Sciences, Faculty of Geosciences, Utrecht University, The Netherlands.

Holotype: Plate IX, figs. a–f. sample KR22S2Y23, slide 1, EF: C14. Utrecht University.

Paratype 1: Plate X, figs. a–f., sample KR22S2Y23, slide 1, EF: R19. Utrecht University.

Paratype 2: Plate XII, figs. a–f., sample KR22S2Y29, slide 2, EF: R29/1. Utrecht University.

Studied material: Karaburun section, NE Turkey, subsection KR22-S2 of Kaya et al., 2025 (samples KR22-S1-Y8 through KR22-S3-Y17) and the Priabonian paratype Bressana section from NE Italy (cf. Brinkhuis, 1994).

Type locality and horizon: İhsaniye Formation, Karaburun section, NW Turkey, sample KR22-S2-Y23, level 53,50 m (=S2, 18,50 m) cf. Kaya et al., 2025.

Age: early Rupelian. **Calibration:** Calcareous nannoplankton zone top NP21/base NP22 (Kaya et al., 2025), and Rac Zone of Brinkhuis and Biffi (1993; this paper).

Diagnosis: An intermediate to large-sized species of *Glaphyrocysta* characterized by having penitabular, distally flared ornamentation on the apical, dorsal and antapical sides, and mixed, partly penitabular, and partly distally complexly connected ornamentation on the ventral side.

Description:

Shape: Endophragm: dorso-ventrally compressed, lenticular to (sub)spherical with two antapical lobes, as typical for most Areoligeraceans. Periphragm: notably on the dorsal and antapical sides giving rise to peni- to quasi-intratubular processes, distally open and flared, while the central ventral side is appressed to the endophragm. Processes distally complexly connected along the margins of the ventral side.

Wall relationships: The walls are composed of an endophragm and a periphragm, the latter giving rise to large apical, dorsal and antapical peni- to quasi-intratubular, distally flared and perforated, indented, open processes. This while the processes along the margins of the ventral are distally connected, eventually grading towards the distal central ventral area into a finely or coarsely ramified, complex ‘network’ of connected strands but leaving the central ventral (i.e. the parasulcal) region open, where the periphragm is appressed to the endophragm.

Wall features: Endophragm: smooth. Periphragm, where appressed to the endophragm microgranulate to microreticulate,

Processes: The dorsal and marginal ventral sides are characterized by large peni- to quasi-intratubular processes, distally open and flared (to distally eventually finely ramified and complexly connected towards the parasulcal area), while at the ventral side both walls are appressed.

Paratabulation: Indicated by most larger processes and the

archaeopyle margin, all typical Areoligeracean, with an ‘offset’ sulcal notch.

Archeopyle: Formed by the release of all the apical paraplates (tA, compound); distinctly angular, with the classic Areoligeracean ‘zigzag’ margin, and an ‘offset’ sulcal notch. The paraplates reflecting 2’ and 3’ are much larger than 1’ and 4’. The operculum is usually detached and has four peni- to quasi intratubular hollow, distally open, flared processes (e.g., Plate XI, figs. e–g).

Paracingulum: Position clearly marked by the margins of the penitabular processes, notably so on the ventral side, but without traces of tabulation.

Parasulcus: Marked by the central ventral region of appressed walls, but without traces of tabulation.

Dimensions: Central body length: 54–64 µm (holotype, 60 µm); width: 62–75 µm (holotype, 66 µm). Overall length/width: 65 × 115 µm (holotype, 93 × 106 µm). Twenty specimens were measured.

Stratigraphic range/occurrence: Early Rupelian.

Comparison: The rather large, distally flared, and irregularly terminating dorsal and marginal penitabular processes are reminiscent of the ornamentation of the morphologically closely related species *Areoligera sentosa*, *A. undulata* and even *A. tauloma* (all of Eaton, 1976, from the Lutetian and Bartonian of the UK). *Glaphyrocysta peterbijlii* differs by having ventrally distally complexly connected processes, also a defining character for assigning it to the genus *Glaphyrocysta*. It is somewhat comparable to the connections in *Glaphyrocysta intricata* (see e.g., Figure Plate XVI), occurring in coeval deposits at Karaburun but differs by truly interconnecting sets of intratubular processes. The large, flared processes also resemble the ornamentation of the classic Oligocene genus *Chiropteridium* (although Eocene varieties have been described as well). These differ in not having penitabular, nor distally connected processes. In this sense, *G. peterbijlii* makes for a fascinating case, morphologically matching criteria for all of the above, sitting right at the onset of the Oligocene. In terms of overall morphology and stratigraphic occurrence, *G. peterbijlii* is also somewhat similar to forms described by Gerlach (1961) as *Cyclonephelium reticulosum* (now *Glaphyrocysta reticulosa*) from the Lower Oligocene of NW Germany. Yet, from the original description, and (rather vague) picture of the holotype, that species is characterized by much more consistently distally complexly ramified processes, and lack of penitabular, distally open, flared (not connected) outgrowths.

Declaration of competing interest

The authors declare that they have no conflict of interest.

Acknowledgments

We thank Natasja Welters and Giovanni Dammers (Geolab, Utrecht University) for palynological processing and Dr. Gea Zijlstra (Utrecht University) for advice regarding the nomenclature of the newly described taxa. We also thank Appy Sluijs and yyy for their constructive and detailed reviews of the originally submitted version of this work. This project is funded by TÜBITAK-2236 fellowship and Horizon 2020 Marie Skłodowska-Curie COFUND action (Project no: 121C058, to M.Y. Kaya).

Appendix A. Supplementary data

Supplementary data to this article can be found online at <https://doi.org/10.1016/j.revpalbo.2025.105414>.

Data availability

The authors confirm that all data necessary for supporting the scientific findings of this paper have been provided.

References

- Agnini, C., Backman, J., Boscolo-Galazzo, F., Condon, D.J., Fornaciari, E., Galeotti, S., Giusberti, L., Grandesso, P., Lanci, L., Luciani, V., Monechi, S., Muttoni, G., Pällike, H., Pampaloni, M.L., Papazzoni, C.A., Pearson, P.N., Pignatti, J., Premoli Silva, I., Raffi, I., Rio, D., Rook, L., Sahy, D., Spofforth, D.J.A., Stefani, C., Wade, B.S., 2021. Proposal for the Global Boundary Stratotype Section and Point (GSSP) for the Priabonian Stage (Eocene) at the Alano section (Italy). *Episodes* 44 (2), 151–173.
- Bati, Z., 2015. Dinoflagellate cyst biostratigraphy of the upper Eocene and lower Oligocene of the Kirmizitepe Section, Azerbaijan, South Caspian Basin. *Rev. Palaeobot. Palynol.* 217, 9–38.
- Bati, Z., Sancay, R.H., 2007. Palynostratigraphy of Rupelian sediments in the Mus Basin, Eastern Anatolia, Turkey. *Micropaleontology* 53 (4), 249–283 text-figures 1–9, plates 1–12, table 1, 2007.
- Bijl, P.K., Brinkhuis, H., Egger, L.M., Eldrett, J.S., Frieling, J., Grothe, A., Houben, A.J.P., Pross, J., Śliwińska, K.K., Sluijs, A., 2016. Comment on 'Wetzeliella and its allies – the 'hole' story: a taxonomic revision of the Paleogene dinoflagellate subfamily Wetzelielloideae' by Williams et al. (2015). *Palynology* 1-7. <https://doi.org/10.1080/01916122.2016.1235056>.
- Brinkhuis, H., 1994. Late Eocene to Early Oligocene dinoflagellate cysts from the Priabonian type-area (Northeast Italy): biostratigraphy and palaeoenvironmental interpretation. *Palaeogeogr. Palaeoclimatol. Palaeoecol.* 107, 121–163.
- Brinkhuis, H., Biffi, U., 1993. Dinoflagellate cyst stratigraphy of the Eocene/Oligocene transition in central Italy. *Mar. Micropaleontol.* 22, 131–183.
- Brinkhuis, H., Visscher, H., 1995. The upper boundary of the Eocene Series; a reappraisal based on dinoflagellate cyst biostratigraphy and sequence stratigraphy. In: Berggren, W.A., Kent, D.V., Aubry, M.-P., Hardenbol, J. (Eds.), *Geochronology, Time Scales and Global Stratigraphic Correlation*, Spec. Publ. Soc. Econ. Palaeontol. Mineral. (SEPM; Soc. Sedimentary Geology), 54, pp. 295–304.
- Bujak, J.P., 1980. Dinoflagellate cysts and acritarchs from the Eocene Barton Beds of southern England. In: Bujak, J.P., Downie, C., Eaton, G.L., Williams, G.L. (Eds.), *Dinoflagellate Cysts and Acritarchs from the Eocene of Southern England*, Special Papers in Palaeontology. The Palaeontological Association, London.
- Eaton, G.L., 1976. Dinoflagellate cysts from the Bracklesham Beds (Eocene) of the Isle of Wight, southern England. *Bull. Brit. Mus (Nat. Hist.) Geol.* 26, 227–332.
- Evitt, W.R., 1985. Sporopollenin dinoflagellate cysts: their morphology and interpretation. American Association of Stratigraphic Palynologists Foundation, Dallas, USA, p. 333pp.
- Fensome, R.A., Taylor, F.J.R., Norris, G., Sarjeant, W.A.S., Wharton, D.I., Williams, G.L., 1993. A classification of fossil and living dinoflagellates. *Micropaleontology*, Special Publication 351.
- Fensome, R.A., Guerin, G.R., Williams, G.L., 2006. New Insights on the Paleogene Dinoflagellate Cyst Genera *Enneadocysta* and *Licracysta* gen. nov. Based on Material from Offshore Eastern Canada and Southern Argentina. *Micropaleontology* 52 (5), 385–410. <https://www.jstor.org/stable/4499750>.
- Gerlach, E., 1961. Mikrofossilien aus dem Oligozän und Miozän Nordwestdeutschlands, unter besonderer Berücksichtigung der Hystrichosphären und Dinoflagellaten. *Neues Jahrb. Geol. Palaontol. Abh.* 112, 143–228 pl. 5.
- Heilmann-Clausen, C., Van Simaey, S., 2005. Dinoflagellate cysts from the Middle Eocene to ?lowermost Oligocene succession in the Kysing Research Borehole, central Danish Basin. *Palynology* 29, 143–204 pl. 1–15.
- Hooker, J.J., King, C., 2019. The Bartonian unit stratotype (S. England): assessment of its correlation problems and potential. *Proc. Geol. Assoc.* 130 (2019), 157–169.
- Houben, A.J.P., et al., 2011. The Eocene–Oligocene transition: changes in sea level, temperature or both? *Palaeogeogr. Palaeoclimatol. Palaeoecol.* <https://doi.org/10.1016/j.palaeo.2011.04.008>.
- Hutchinson, D.K., et al., 2021. The Eocene–Oligocene transition: a review of marine and terrestrial proxy data, models and model–data comparisons. *Clim. Past* 17 (269–315), 2021. <https://doi.org/10.5194/cp-17-269-2021>.
- Hyland, E., Murphy, B., Varela, P., Marks, K., Colwell, L., Tori, Fl., Monechi, S., Cleaveland, L., Brinkhuis, H., van Mourik, C.A., Coccioni, R., Bice, D., Montanari, A., 2009. Integrated stratigraphic and astrochronologic calibration of the Eocene–Oligocene transition in the Monte Cagnero section (northeastern Apennines, Italy): a potential parastratotype for the Massignano global stratotype section and point (GSSP). In: Koerber, C., Montanari, A. (Eds.), *The Late Eocene Earth—Hothouse, Icehouse, and Impacts*, Geological Society of America Special Paper, 452, pp. 303–322. [https://doi.org/10.1130/2009.2452\(19\)](https://doi.org/10.1130/2009.2452(19)).
- Iakovleva, A.I., 2025. Organic walled dinoflagellate cyst biostratigraphy of the Bartonian/Priabonian GSSP Alano di Piave section, NE Italy. *Rev. Palaeobot. Palynol.*, 105233 <https://doi.org/10.1016/j.revpalbo.2024.105233>.
- Iakovleva, A.I., Zakrevskaya, E.Y., Shcherbinina, E.A., 2024. Middle Eocene to earliest Oligocene dinoflagellate cysts from southern Armenia: biostratigraphy and palaeoecology. *Palynology* 48 (3). <https://doi.org/10.1080/01916122.2024.2343902>.
- Kaya, M.Y., Brinkhuis, H., Fioroni, C., Atasoy, S.G., Licht, A., Nürnberg, D., Vural, T., 2025. The Eocene–Oligocene Transition in the paratethys: boreal water ingression and its paleoceanographic implications. *EGUphere*. <https://doi.org/10.5194/egusphere-2025-479>.
- Köthe, A., 1990. Paleogene dinoflagellates from Northwest Germany - biostratigraphy and paleoenvironment. *Geol. Jahrb.*, A, 118, p. 111.
- Morgenroth, P., 1966. Neue in organischer Substanz erhaltene Mikrofossilien des Oligozäns. *Neues Jahrb. Geol. Palaontol. Abh.* 127, 1–12.
- The Eocene–Oligocene Boundary in the Marche–Umbria Basin (Italy). In: Premoli Silva, I., Coccioni, R., Montanari, A. (Eds.), 1988. IUGS Special Publication: Ancona, Italy. Fratelli Aniballi Publishers, pp. 137–161.
- Pross, J., Houben, A.J.P., Van Simaey, S., Williams, G.L., Kothhoff, U., Coccioni, R., Wilpshaar, M., Brinkhuis, H., 2010. Umbria–Marche revisited: a refined magnetostratigraphic calibration of dinoflagellate cyst events for the Oligocene of the Western Tethys. *Rev. Palaeobot. Palynol.* 158, 213–235.
- Sancay, R.H., Bati, Z., 2020. Late Eocene to Early Oligocene palynostratigraphy of the Western Black Sea, Eastern Paratethys. *Turk. J. Earth Sci.* 29, 115–138.
- Schiøler, P., 2005. Dinoflagellate cysts and acritarchs from the Oligocene–Lower Miocene interval of the Alma-IX well, Danish North Sea. *J. Micropalaeontol.* 24, 1–37. <https://doi.org/10.1144/jm.24.1.1>.
- Śliwińska, K.K., 2019. Early Oligocene dinocysts as a tool for palaeoenvironment reconstruction and stratigraphical framework – a case study from a North Sea well. *J. Micropalaeontol.* 38, 143–176. <https://doi.org/10.5194/jm-38-143-2019>.
- Stover, L.E., Evitt, W., 1978. R.: *Analyses of Pre-Pleistocene Organic-Walled Dinoflagellates*, Geological Sciences. Stanford University Publications, Stanford, 300 pp.
- Stover, L.E., Hardenbol, J., 1994. Dinoflagellates and depositional sequences in the lower Oligocene (Rupelian) Boom clay formation, Belgium. *Bulletin van de Belgische Vereniging voor Geologie/Bulletin de la Societe belge de Geologie T.* 102, 5–77.
- van Mourik, C.A., Brinkhuis, H., 2005. The Massignano Eocene–Oligocene golden spike section revisited. *Stratigraphy* 2, 13–30.
- van Simaey, S., Munsterman, D., Brinkhuis, H., 2005. Oligocene dinoflagellate cyst biostratigraphy of the southern North Sea Basin. *Rev. Palaeobot. Palynol.* 134 (2005), 105–128.
- Viganò, A., Agnini, C., 2025. Beyond the ice: shifts in productivity and carbonate oversaturation at the Eocene–Oligocene transition. *Sci. Rep.* 15 (1), 15281.
- Westerhold, T., Marwan, N., Drury, A.J., et al., 2020. An astronomically dated record of Earth's climate and its predictability over the last 66 million years. *Science* 369 (6509), 1383–1387.
- Williams, G.L., Fensome, A., MacRae, R.A., 2019. *The Lentin and Williams index of fossil dinoflagellates 2019 edition*. American Association of Stratigraphic Palynologists Contributions Series 50, 1173.
- Zachos, J.C., et al., 2001. Trends, rhythms, and aberrations in global climate 65 Ma to present. *Science* 292 (5517), 686–693. <https://doi.org/10.1126/science.1059412>.